Physical Oceanography - UNAM, Mexico
Lecture 1: Introduction to Ocean Circulation

Robin Waldman

October 10th 2018

A first taste...

A wealth of dynamical structures !

A first taste...

A relative decoupling with the atmosphere : a coupled system ? A forced ocean ?

Outline

Outline

Before 1900 : scarce observations

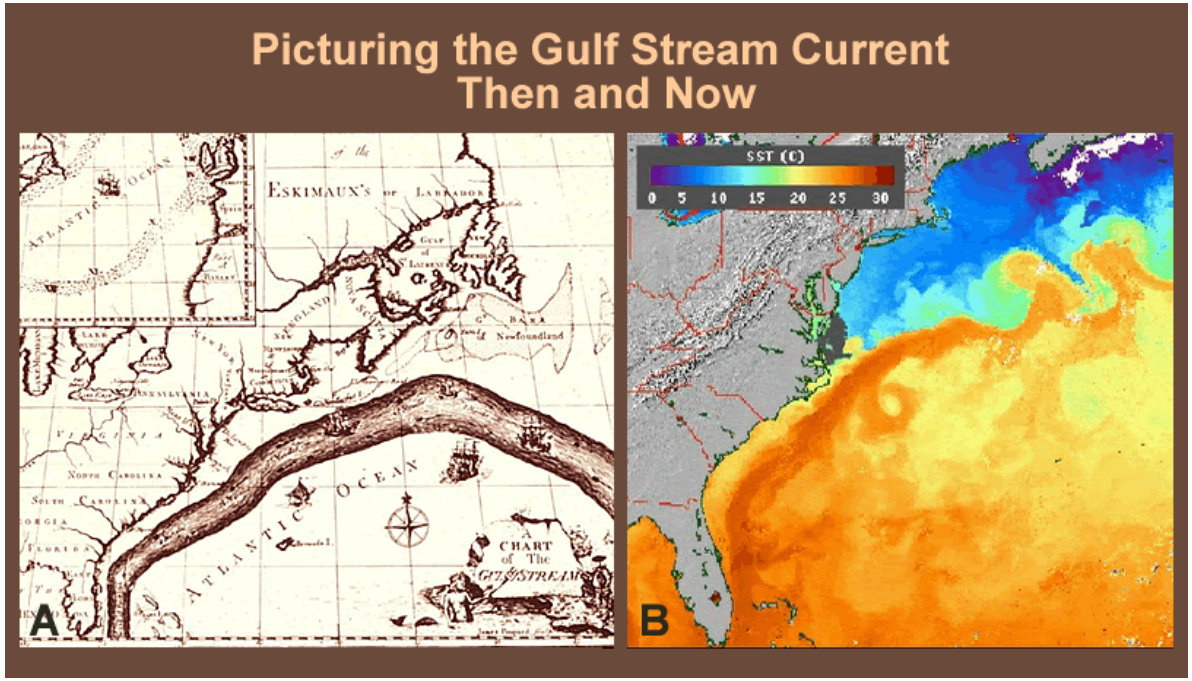

Figure 1 – (a) Estimated Gulf Stream path by Benjamin Franklin (1770) and (b) recent satellite image of sea surface temperature (NOAA).

Before 1900 : scarce observations

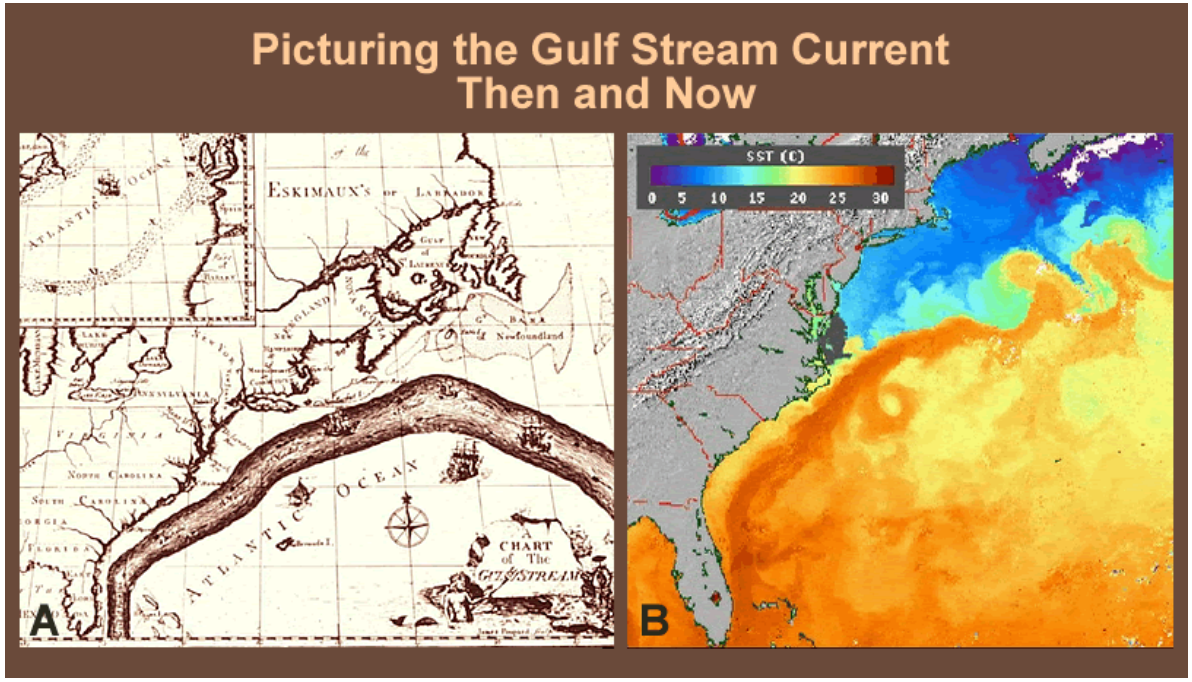

Figure 1 – (a) Estimated Gulf Stream path by Benjamin Franklin (1770) and (b) recent satellite image of sea surface temperature (NOAA).

Sea surface temperature is an excellent indicator of the Gulf Stream's location. Why ?

Before 1900 : scarce observations

The Geostrophic relation :

$$f\mathbf{k} \times \mathbf{u_g} = -\frac{1}{\rho_0} \boldsymbol{\nabla}_h P$$

Problem : pressure gradient is almost unmeasurable in the ocean, still today !

Before the 20th century : scarce observations

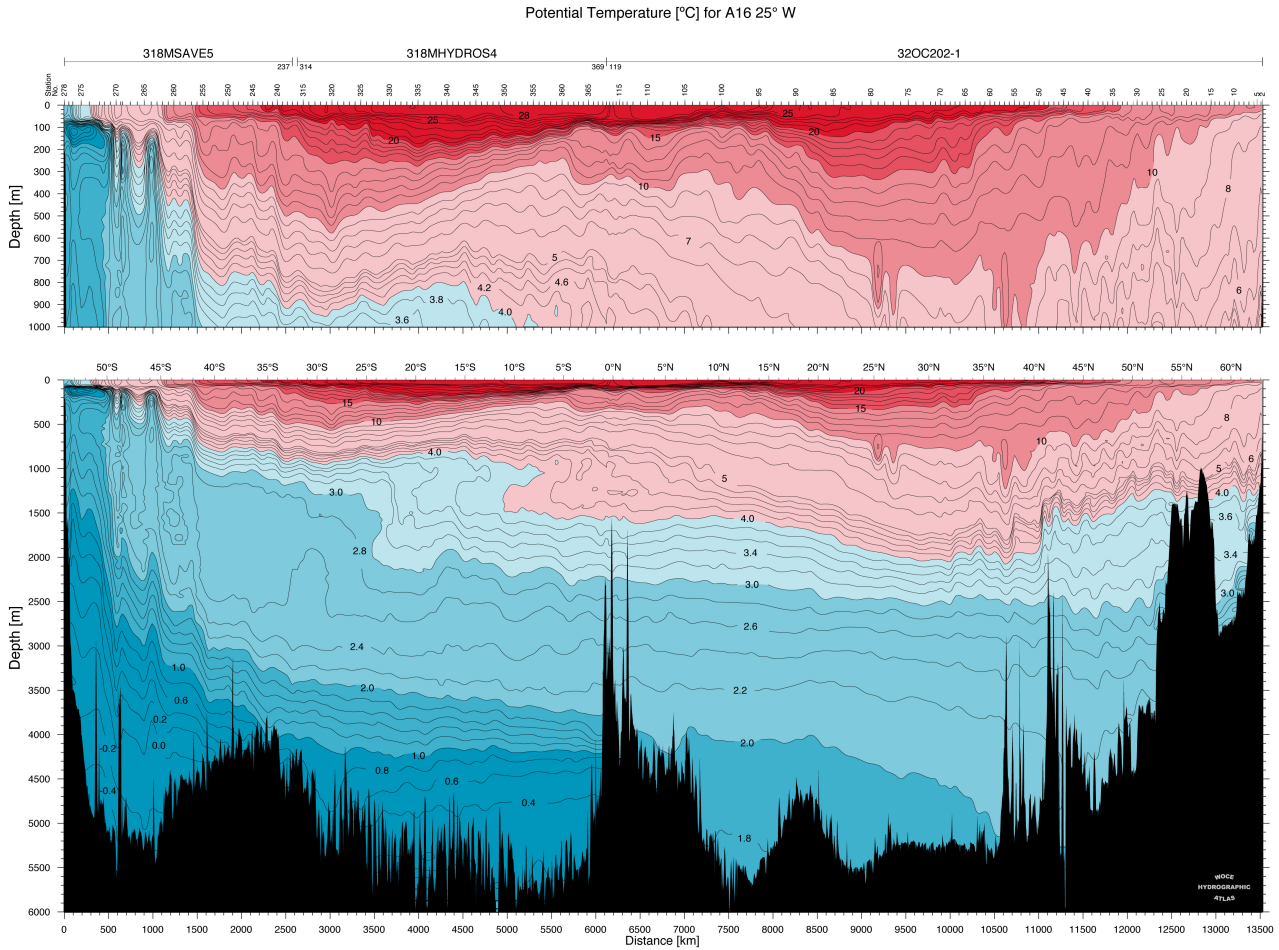

Figure 2 – Meridional potential temperature section in the Atlantic Ocean (WOD 2013).

Before the 20th century : scarce observations

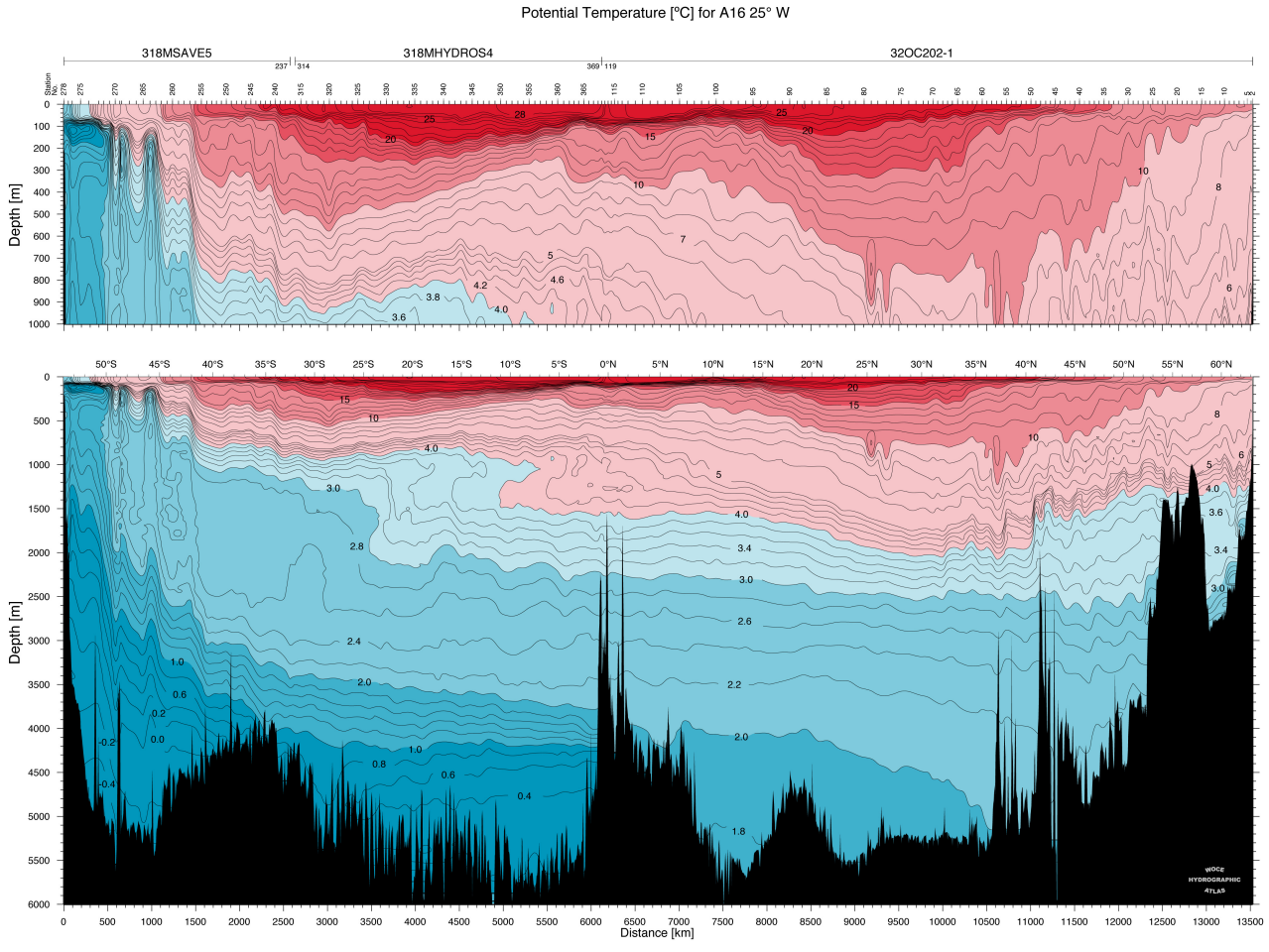

Figure 2 – Meridional potential temperature section in the Atlantic Ocean (WOD 2013).

Below 2000m depth, water masses are colder than $5°C$ at all latitudes.

Early 20th century : first theories

The "Dynamical Method" :

- Hydrostatic relation :

$$\partial_z P = -\rho g$$

- Thus thermal wind relation :

$$\mathbf{k} \times \partial_z \mathbf{u_g} = -\frac{g}{\rho_0 f} \boldsymbol{\nabla}_h \rho$$

- Retrieval of geostrophic currents by vertical integration :

$$\mathbf{u_g}(z) = \mathbf{u_g}(z_r) + \int_{z_r}^{z} \partial_z \mathbf{u_g} dz'$$

Early 20th century : first theories

The "Dynamical Method" :

- Hydrostatic relation :

$$\partial_z P = -\rho g$$

- Thus thermal wind relation :

$$\mathbf{k} \times \partial_z \mathbf{u_g} = -\frac{g}{\rho_0 f} \boldsymbol{\nabla}_h \rho$$

- Retrieval of geostrophic currents by vertical integration :

$$\mathbf{u_g}(z) = \mathbf{u_g}(z_r) + \int_{z_r}^{z} \partial_z \mathbf{u_g} dz'$$

Problem : what reference level z_r and velocity $\mathbf{u_g}(z_r)$ to choose ?

Early 20th century : first theories

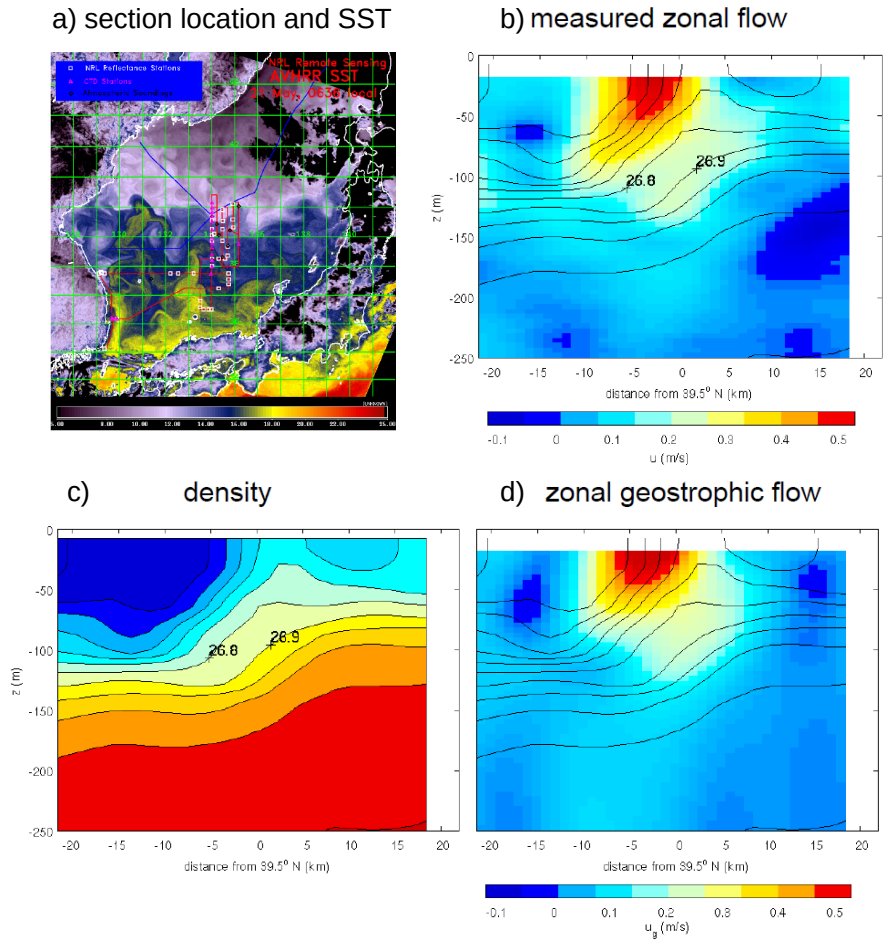

Figure 3 – a) Satellite sea surface temperature, b-c) observed zonal velocities and potential density and d) geostrophic velocities from the "Dynamical Method" (Thomas et al 2010).

Early 20th century : first theories

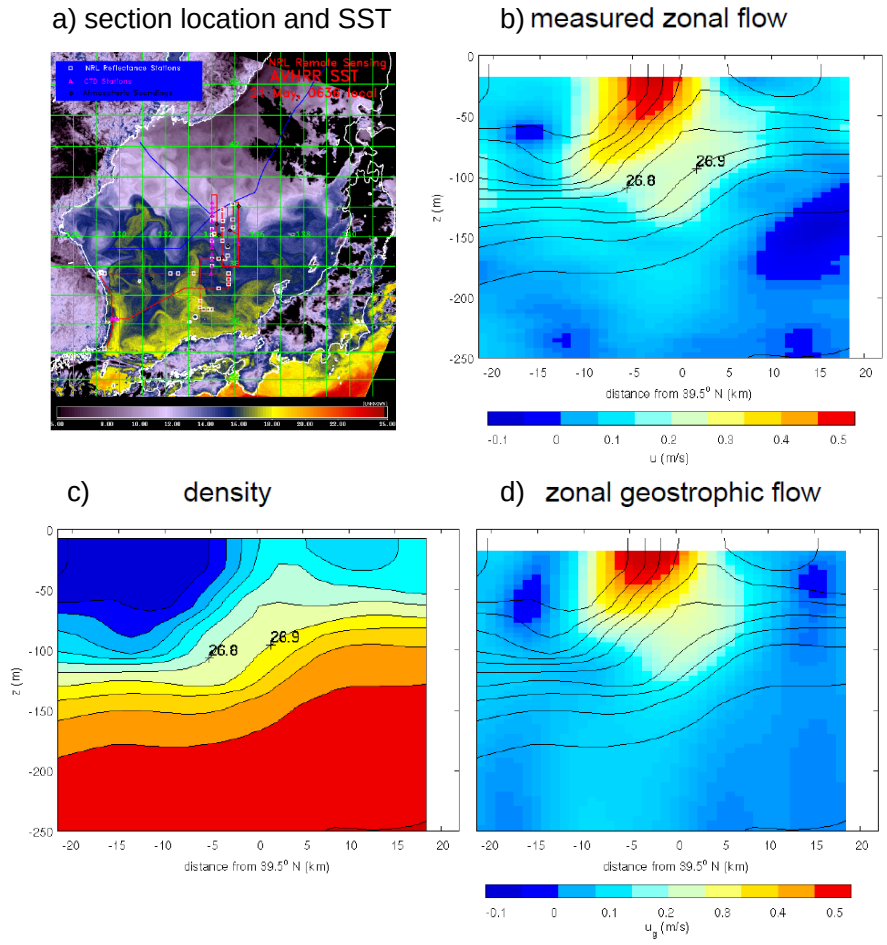

Figure 3 – a) Satellite sea surface temperature, b-c) observed zonal velocities and potential density and d) geostrophic velocities from the "Dynamical Method" (Thomas et al 2010).

Despite the Kuroshio's magnitude and reduced size, it is very well estimated by the geostrophic relation.

Early 20th century : first theories

- Ekman currents :

$$f\mathbf{k} \times \mathbf{U_{eh}} = -\frac{1}{\rho_0}\boldsymbol{\tau}_h$$

Explained why Icebergs drift to the right of winds in the Arctic Ocean !

Early 20th century : first theories

- Ekman currents :

$$f\mathbf{k} \times \mathbf{U_{eh}} = -\frac{1}{\rho_0}\boldsymbol{\tau}_h$$

Explained why Icebergs drift to the right of winds in the Arctic Ocean !

- Sverdrup transports :

$$\beta V = \mathbf{k}.\boldsymbol{\nabla}_h \times \boldsymbol{\tau}_h = Curl(\boldsymbol{\tau}_h)$$

Explained the ocean gyres.

Early 20th century : first theories

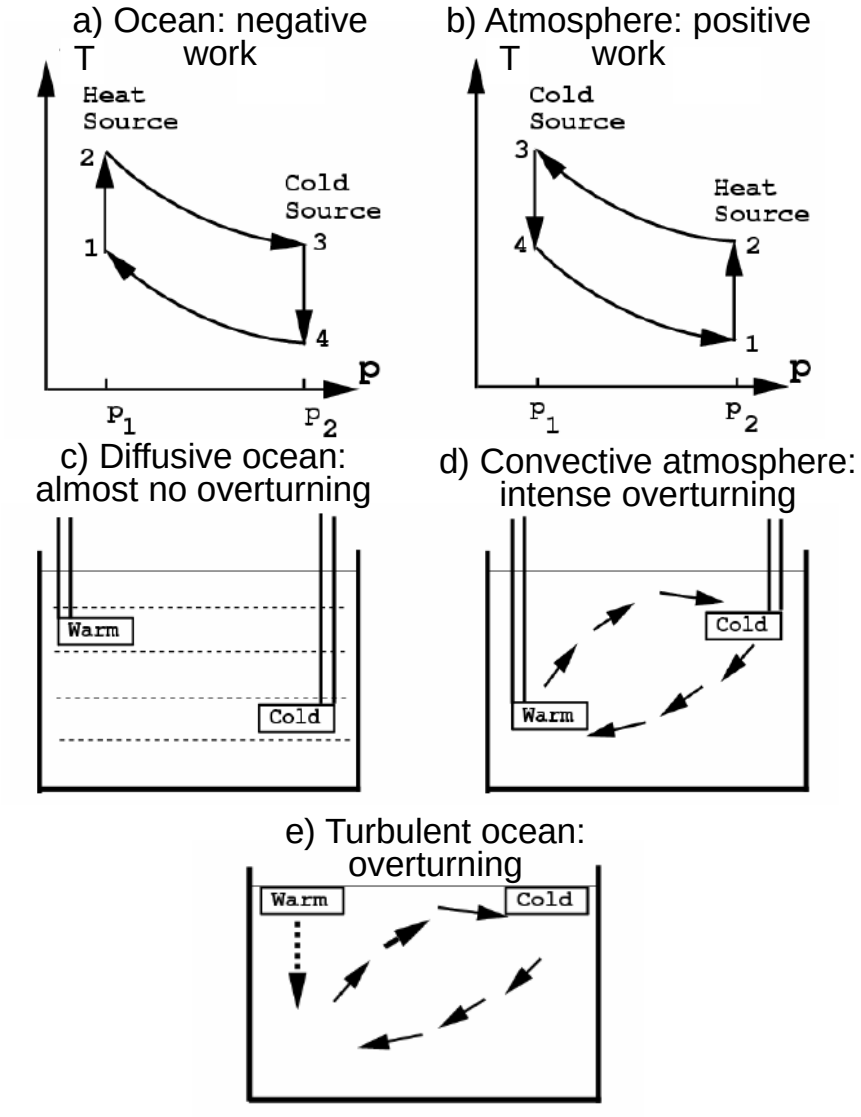

Sandström's "theorem" : an ocean heated from above should display weak overturning.

1940's to 1970's : the era of theoreticians

- Gyre circulation : Munk, Stommel
- Geophysical fluid dynamics : role of topography, baroclinic and barotropic instabilities, etc.
- The "closure of turbulence" : the oceanic mixed layer and air-sea fluxes

But very scarce observations of the ocean and very limited modelling !

Mass observations

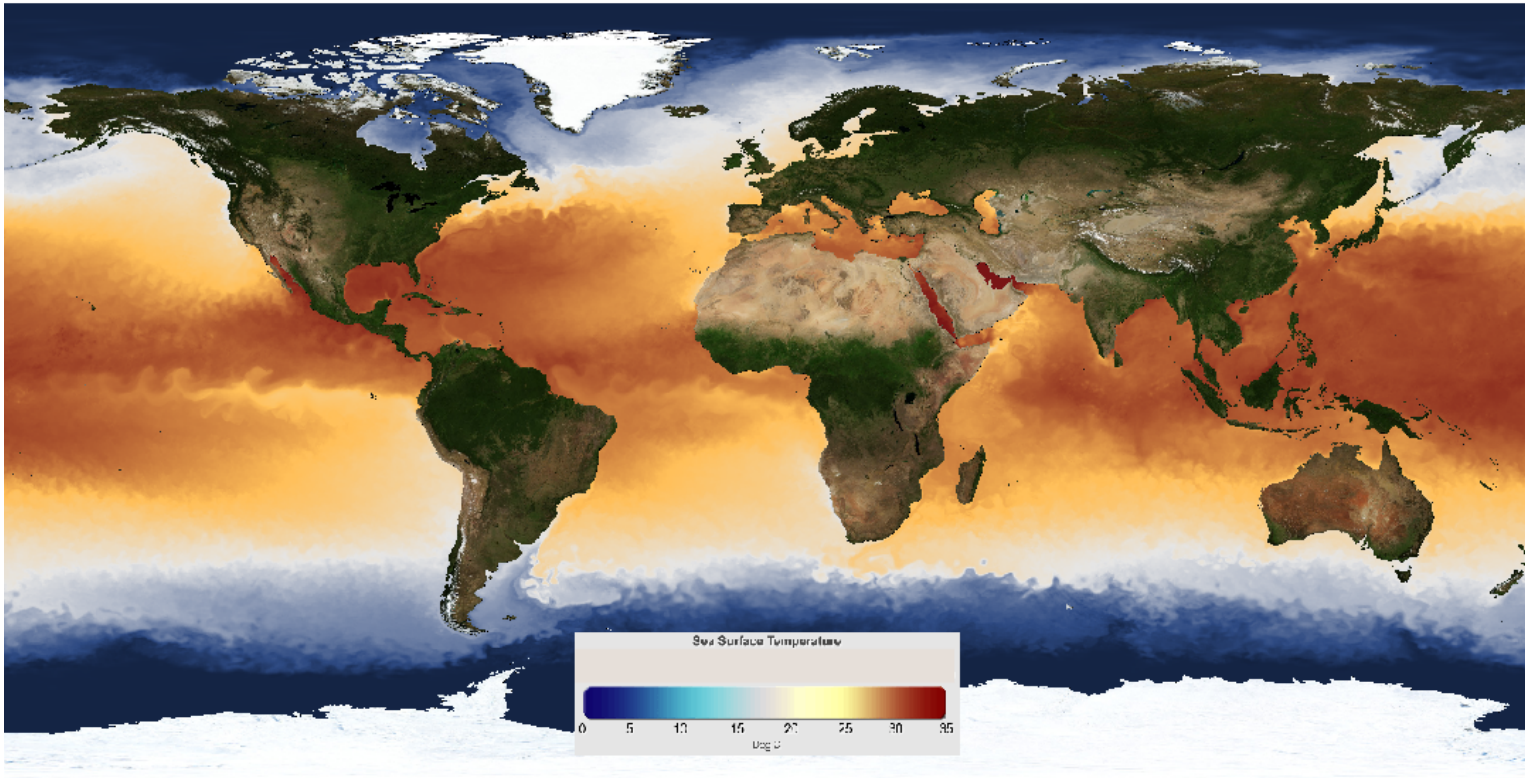

Figure 4 – Near real-time sea surface temperature analysis on Aug. 29th 2018 (NOAA).

- The surface heat content is observable
- It is related to circulation patterns

Mass observations

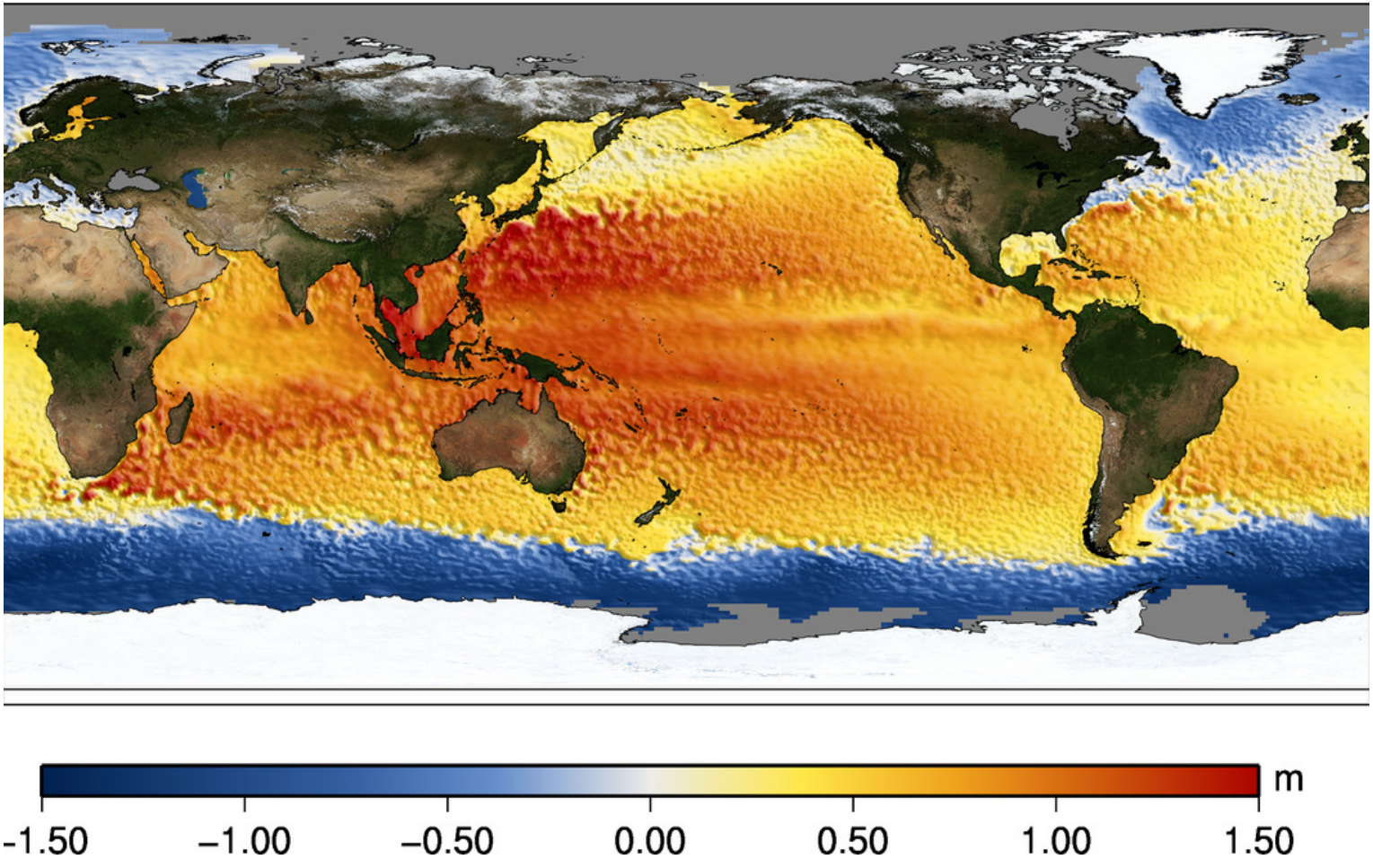

Figure 5 – Dynamic sea level on Dec. 31th 2012 (AVISO).

- Large-scale : gyre circulation
- Small-scale : intense fronts and mesoscale turbulence

Mass observations

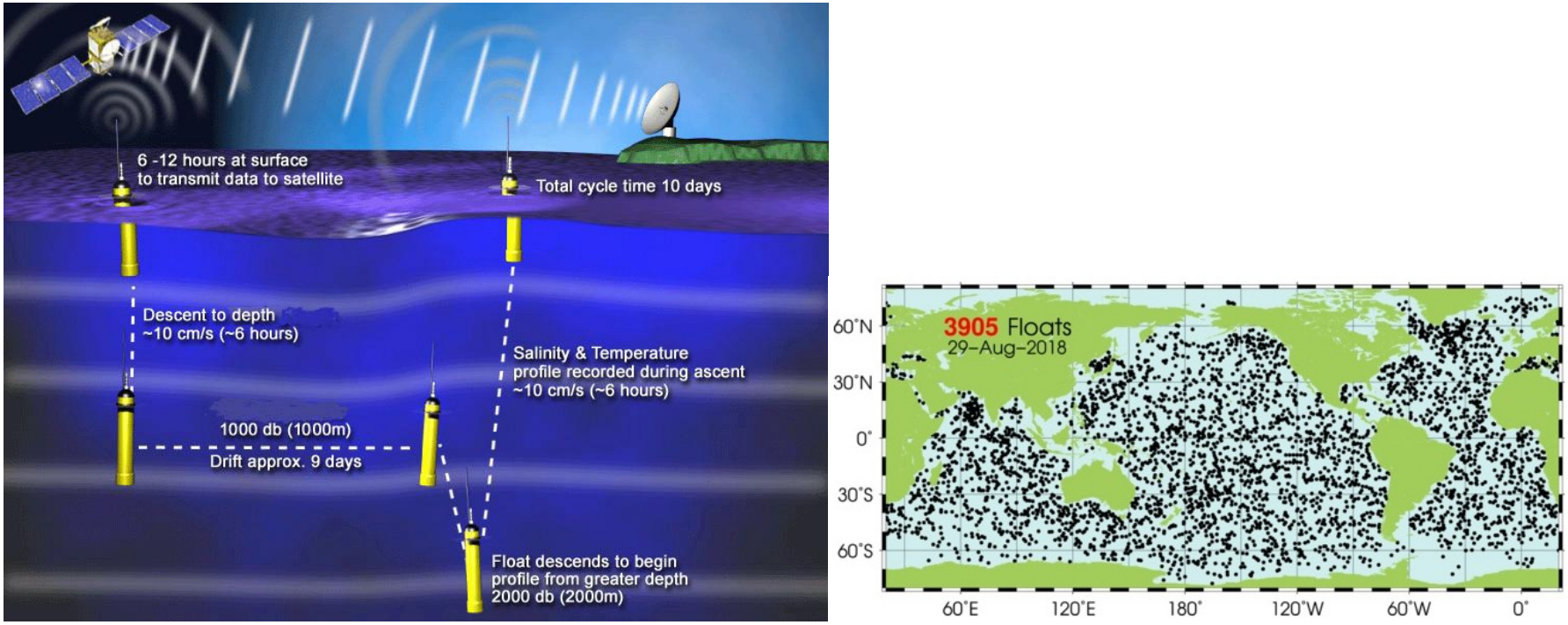

Figure 6 – a) Functioning of an ARGO float and b) the ARGO network on a given day (ARGO database).

- Global coverage
- In situ hydrography + currents at the parking depth

Mass observations

a) Glider functioning cycle

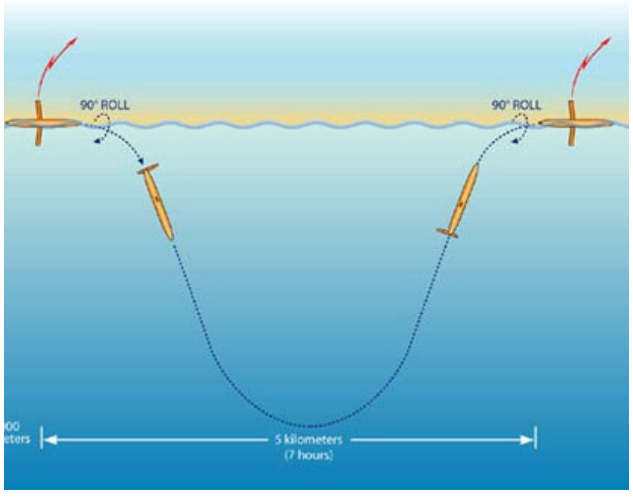

b) Measurement of submesoscale fronts and subduction

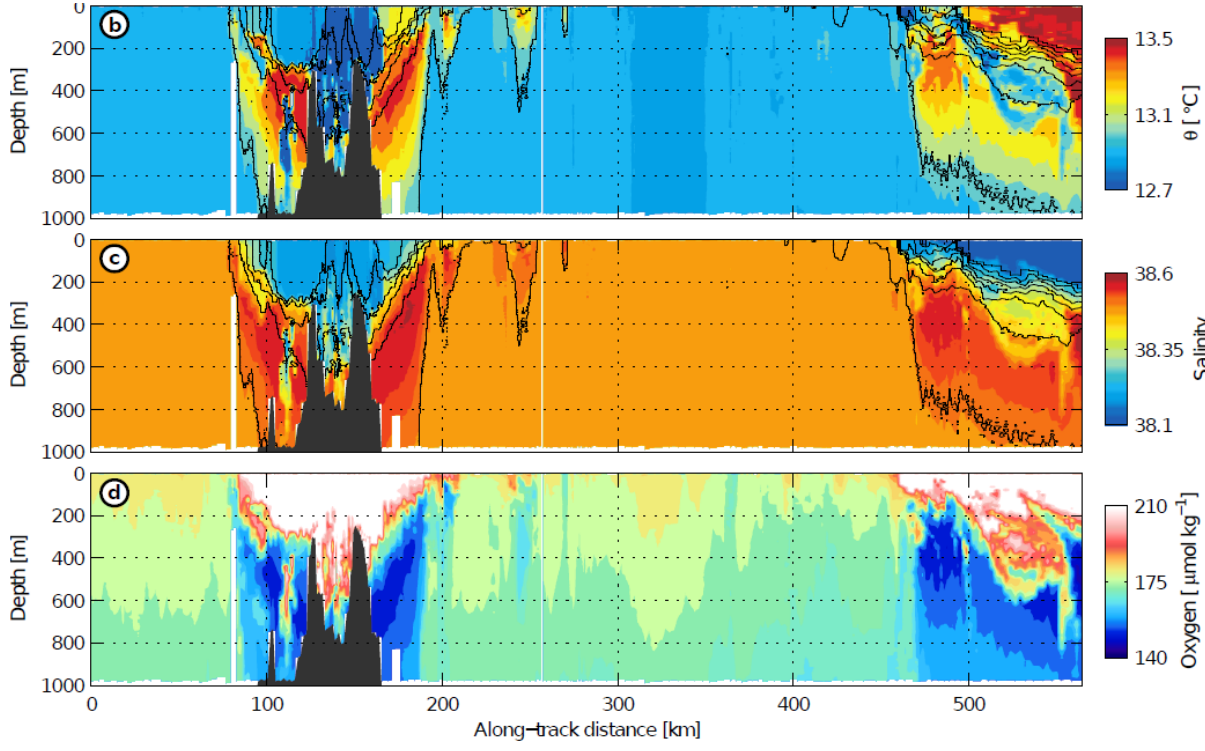

Figure 7 – a) Functioning of a glider and example of a b) potential temperature, c) salinity and d) oxygen concentration section across several fronts in the Mediterranean Sea (A. Bosse's PhD).

- Autonomous drift
- Small-scale in situ observations

Numerical modelling

- Operational oceanography : assimilates observations in numerical models to produce forecasts. Data assimilation is a core aspect of it.

Numerical modelling

- Operational oceanography

a) Currents

b) Sea surface temperature

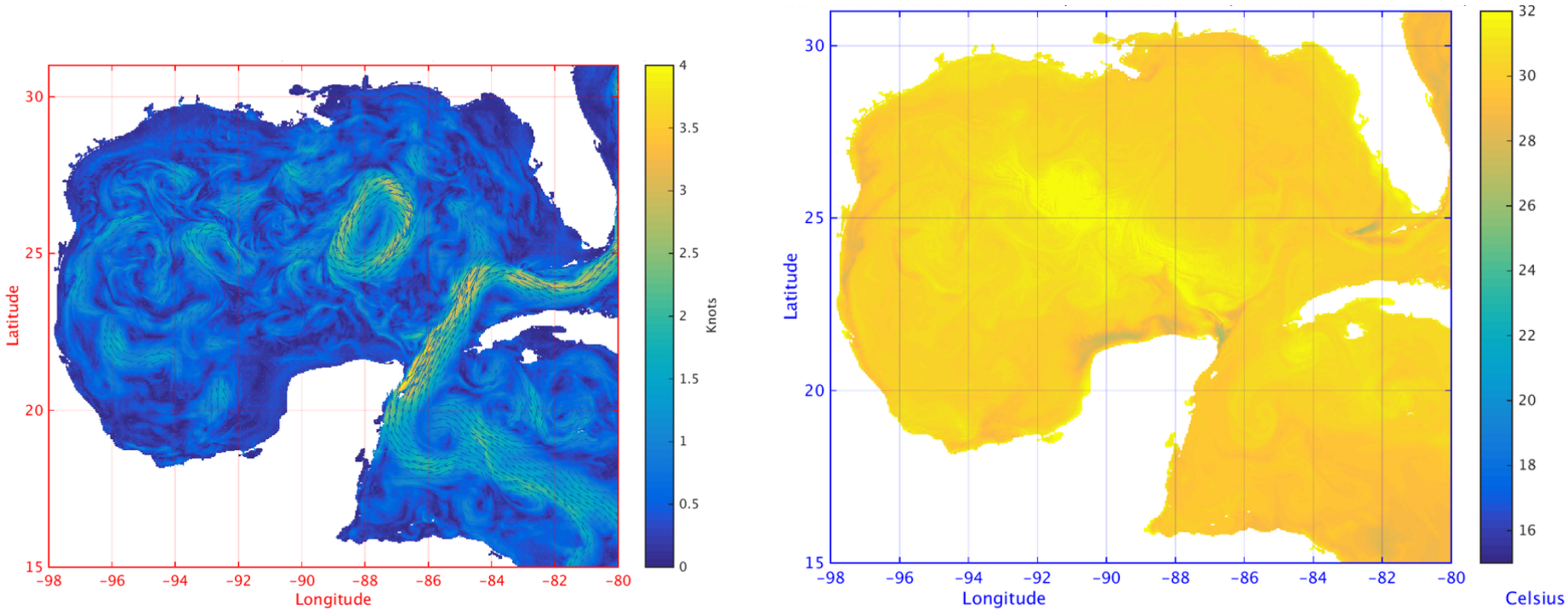

Figure 8 – 4th day surface ocean forecast on Sep. 2nd 2018 for the Gulf of Mexico (NOAA).

Numerical modelling

- Operational oceanography

a) Currents

b) Sea surface temperature

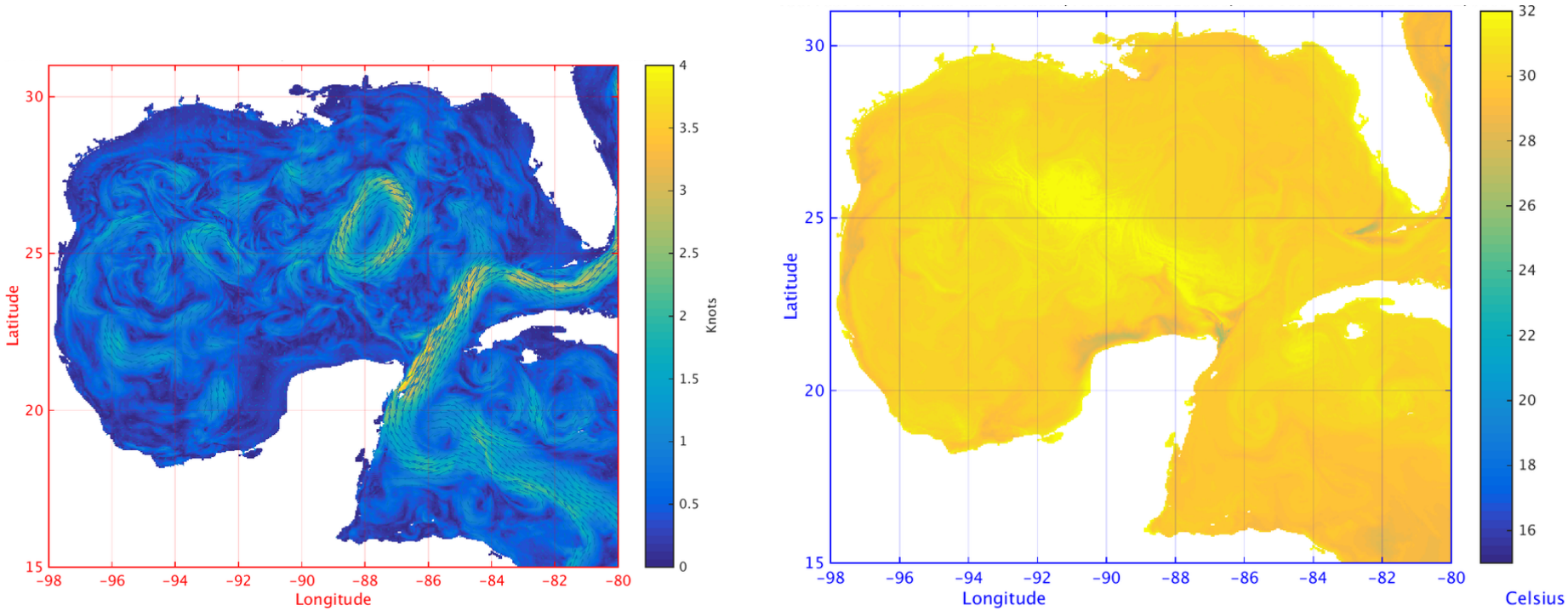

Figure 8 – 4th day surface ocean forecast on Sep. 2nd 2018 for the Gulf of Mexico (NOAA).

- In these maps : Western boundary current, "Loop Current", Yucatán upwelling and eddies

Numerical modelling

- "Coupled physical-biogeochemical" models represent biogeochemical cycles of matter (C, N, P), nutrients and marine biology. Designed for biological applications and challenging computational costs.

Numerical modelling

- Ocean biogeochemistry

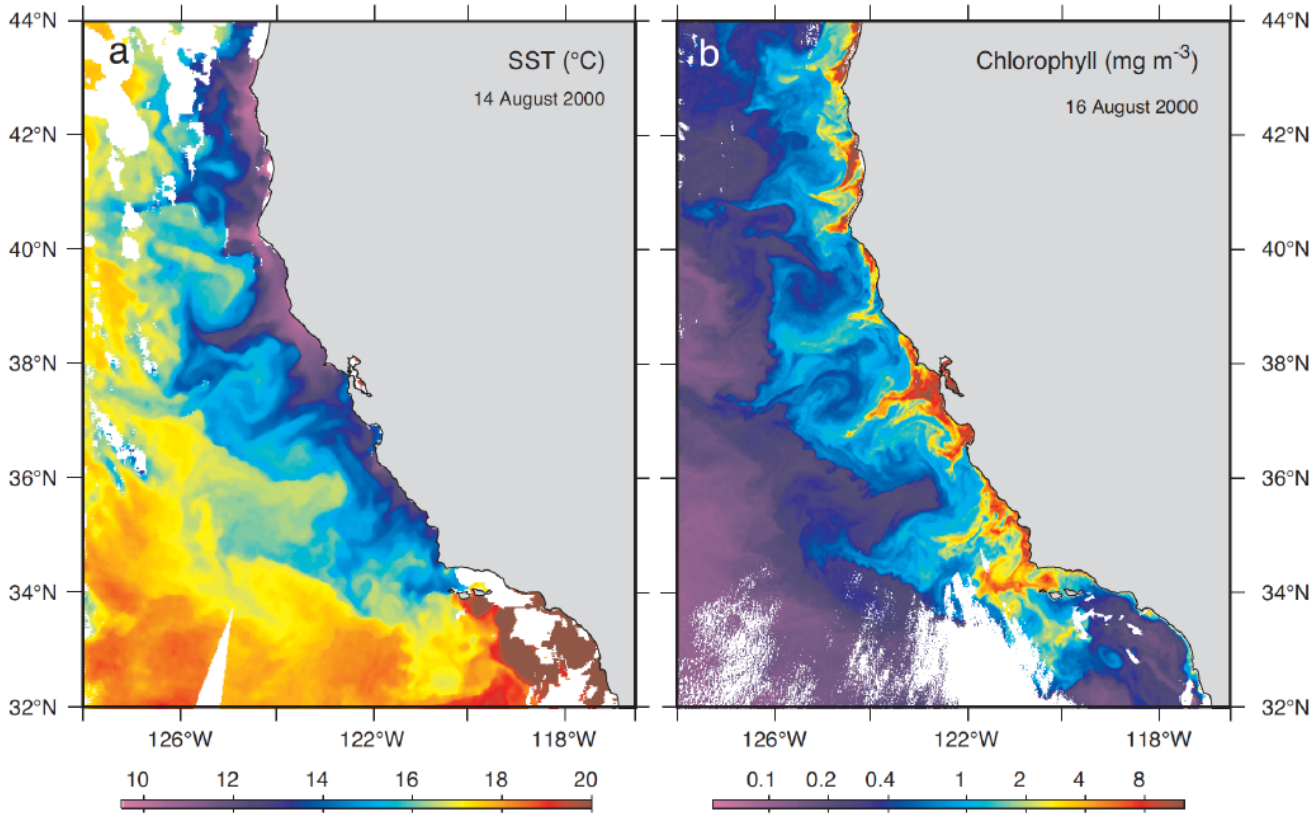

Figure 9 – Sea surface temperature and surface chlorophyll concentration off the US West Coast (Sarmiento and Gruber 2006).

Numerical modelling

- Ocean biogeochemistry

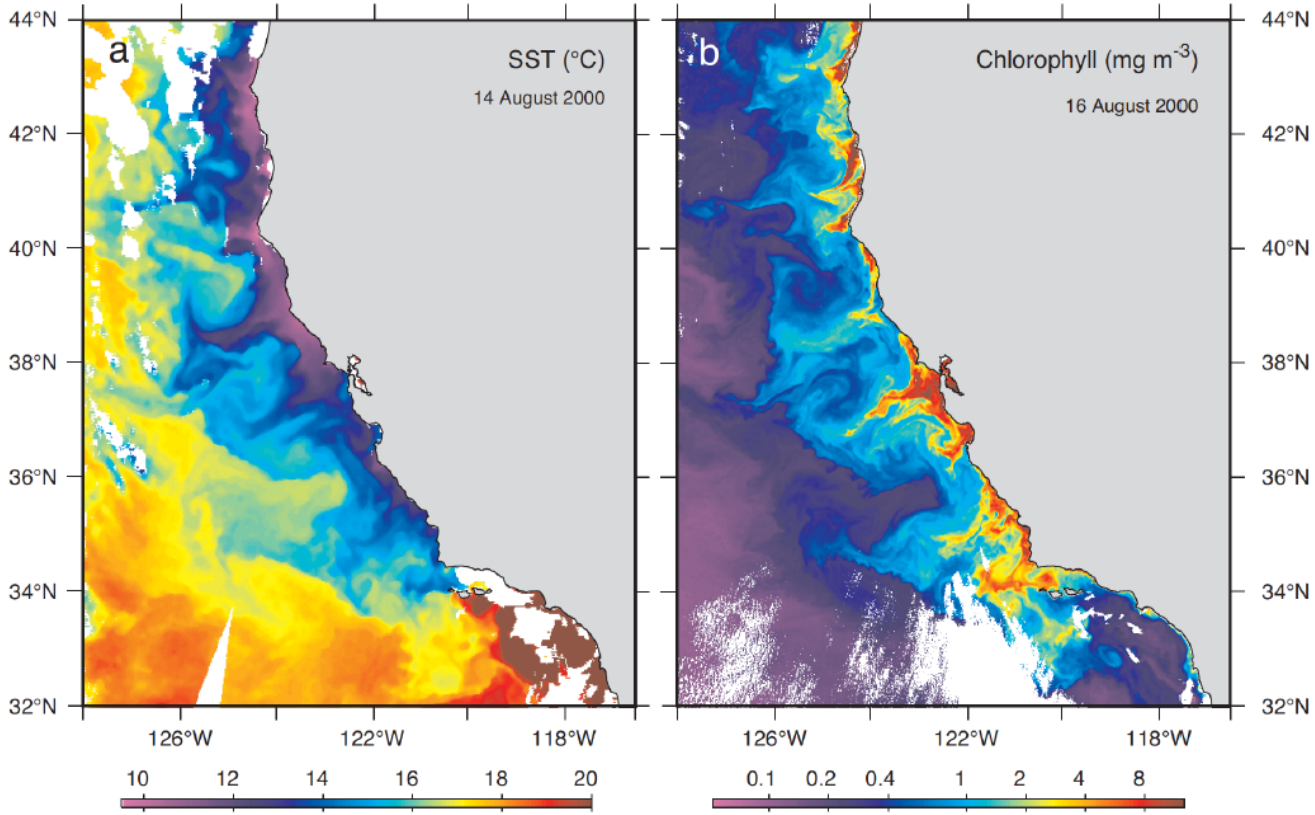

Figure 9 – Sea surface temperature and surface chlorophyll concentration off the US West Coast (Sarmiento and Gruber 2006).

- In these maps : marine biology is very sensitive to ocean physics, and in particular to vertical exchanges.

Numerical modelling

- Coupled ocean-atmosphere models : from operational weather forecasts to long-term climate projections, including sub/seasonal and decadal forecasts. The ocean becomes a compulsory component from subseasonal to climatic timescales.
- "Earth System Models" are climate models that include, in addition to the ocean-atmosphere coupling, the carbon cycle and additional "Earth system" components (e.g. aerosols, interactive land vegetation).

Numerical modelling

- Coupled climate modelling

a) Subpolar North Atlantic sea surface temperature decadal forecast

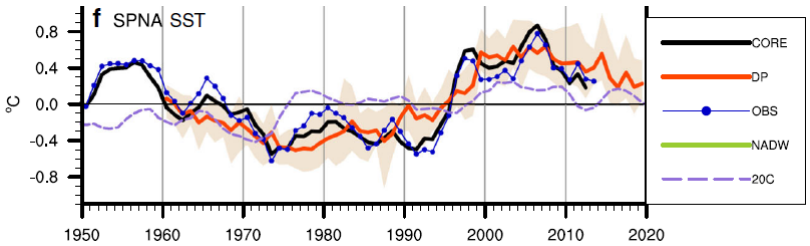

b) Late summer Arctic sea ice extent as a function of global warming

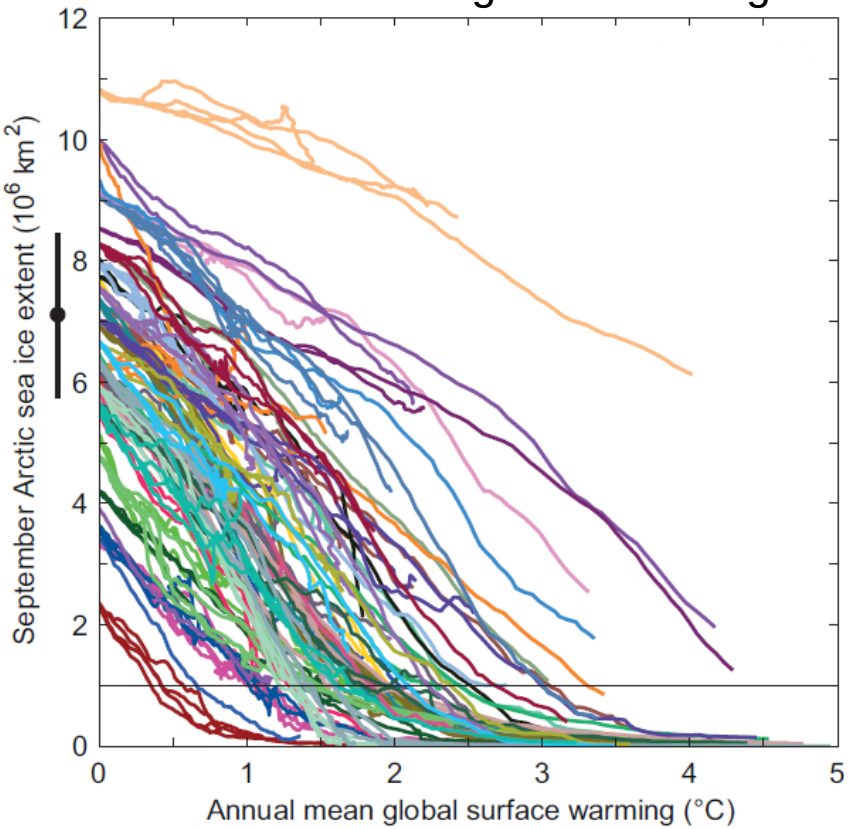

c) 2081-2100 local warming as a function of global warming (°C/°C)

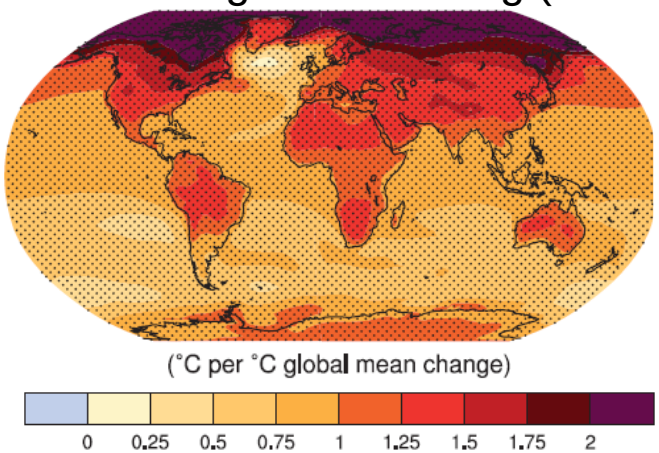

Figure 10 – a) Decadal prediction of sea surface temperature in the Subpolar North Atlantic (Yeager et al 2017), b) climate scenario of the late summer Arctic sea ice extent as a function of global warming and c) 2081-2100 local warming as a function of global warming (IPCC).

Current challenges

a) ARGO network limitations

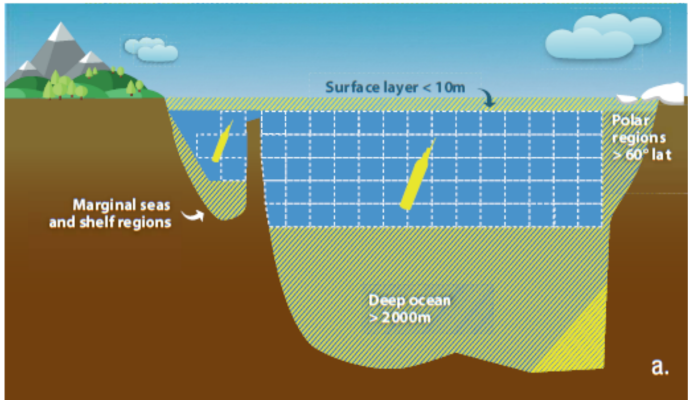

b) ARGO estimated ocean heat content trends

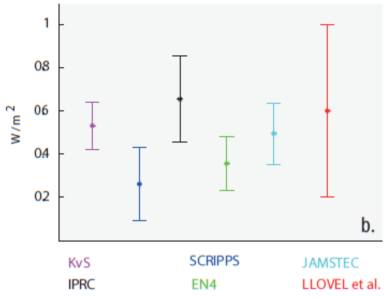

c) In situ observations of oceanic mixing

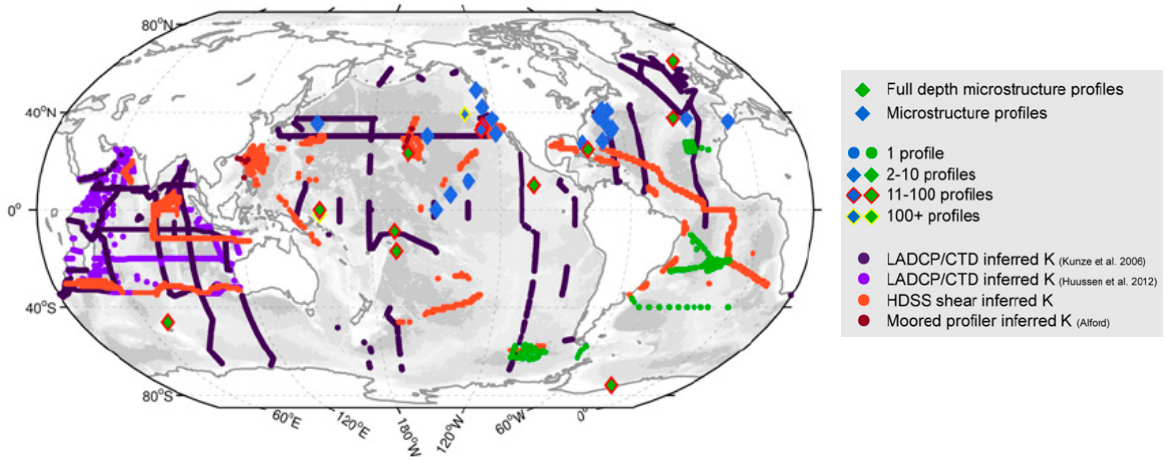

Figure 11 – a) Main ARGO network limitations and b) consequence for the 2006-2012 heat content trend of the upper 2000m (von Schuckmann et al 2016). c) Location of oceanic mixing observations (Waterhouse et al 2014).

Current challenges

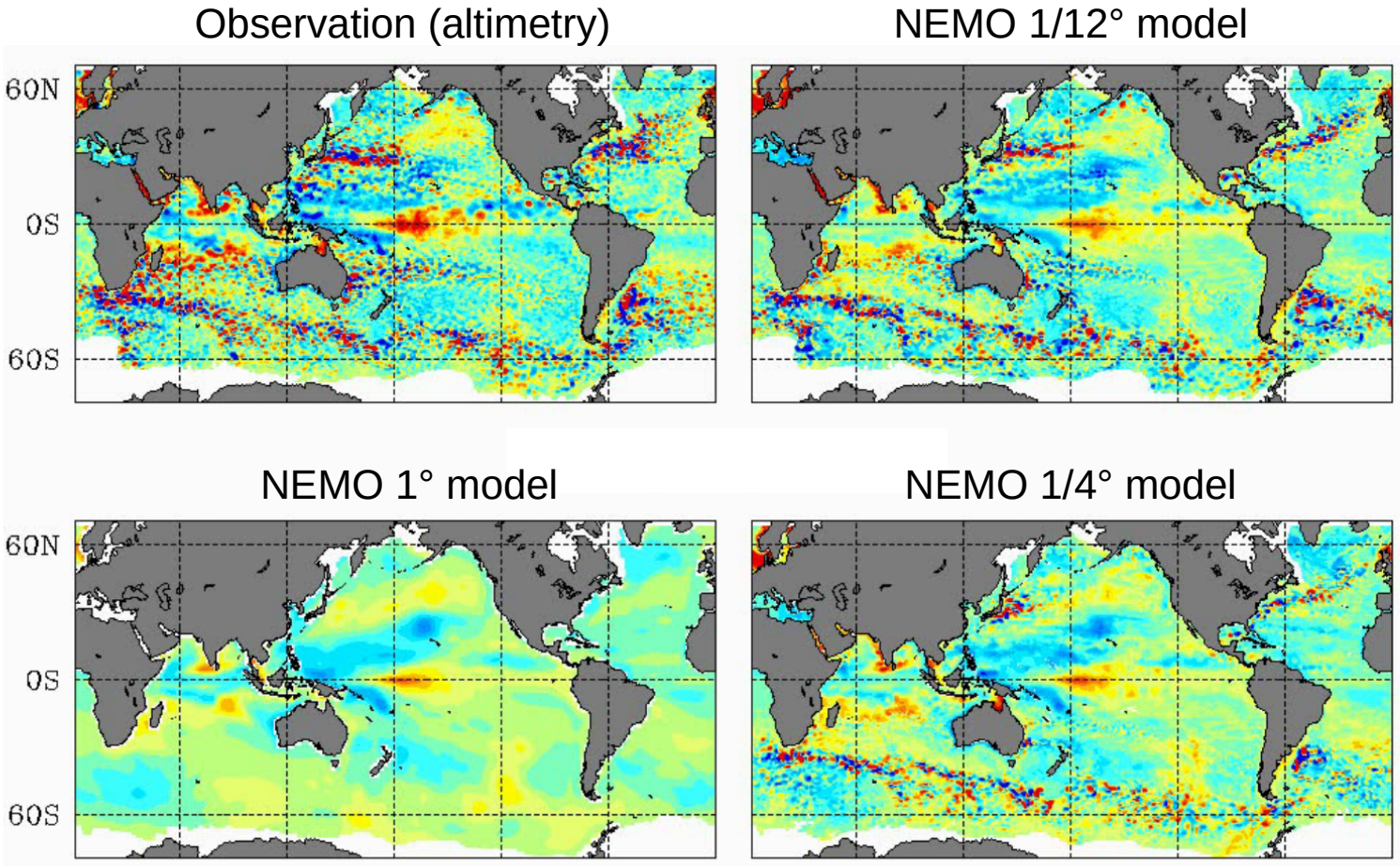

Figure 12 – Sea level anomaly on Jan. 6th 1993 retrieved from observations, a typical short-scale ocean model (NEMO 1/12°), its climate counterpart (NEMO 1°) and an intermediate resolution (NEMO 1/4°).

Outline

Dynamic sea level

Relation between sea level and circulation : the surface geostrophic balance :

$$f\mathbf{k}\times\mathbf{u_{g0}} = -\frac{1}{\rho_0}\boldsymbol{\nabla}_h P = -g\boldsymbol{\nabla}_h \eta$$

By far the main observed dynamical property of the ocean !

Dynamic sea level

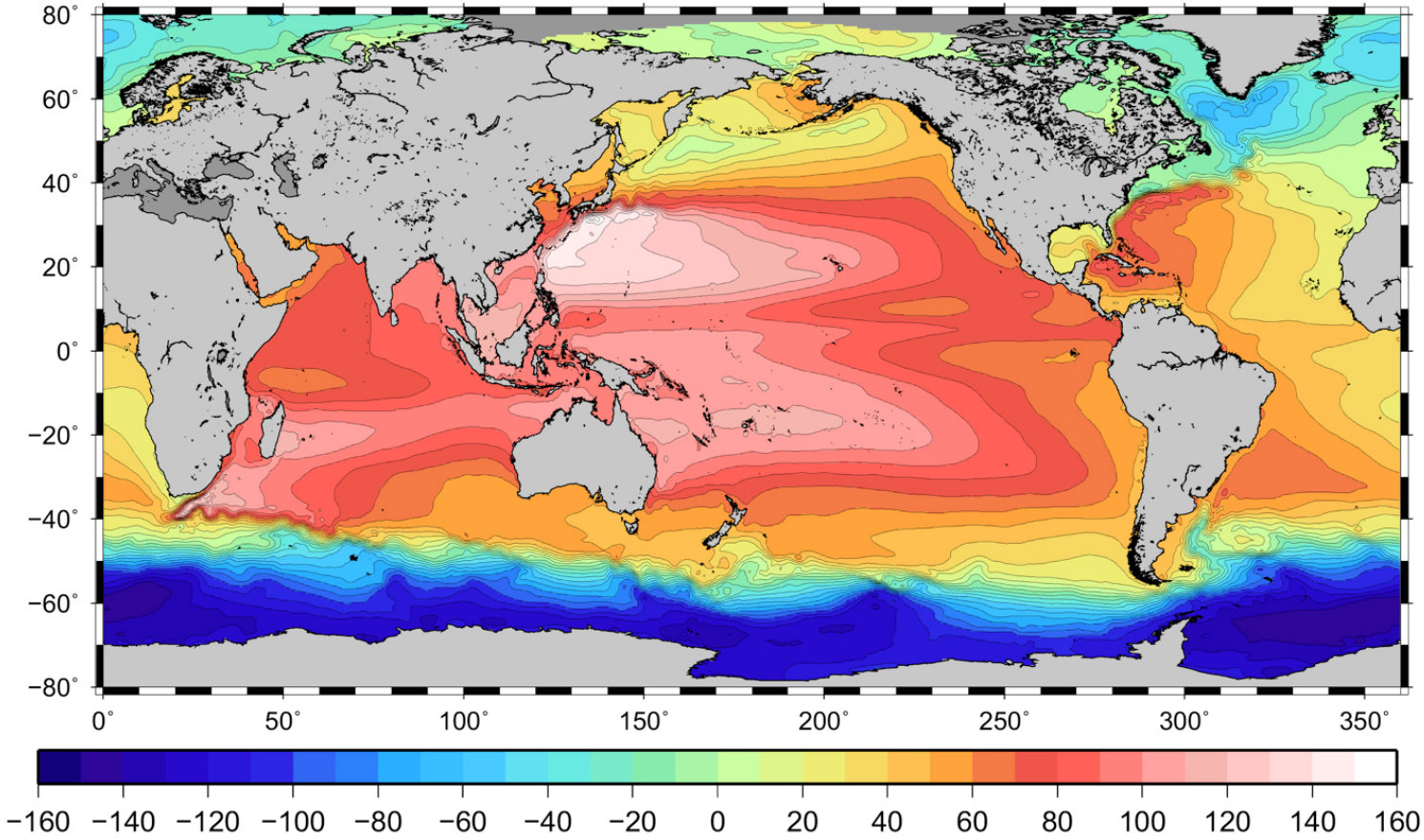

Figure 13 – Mean dynamic topography (cm) deduced from satellite (ESA/CNES/CLS).

- Gyres and the Antarctic Circumpolar Current stand out.

Mass observations

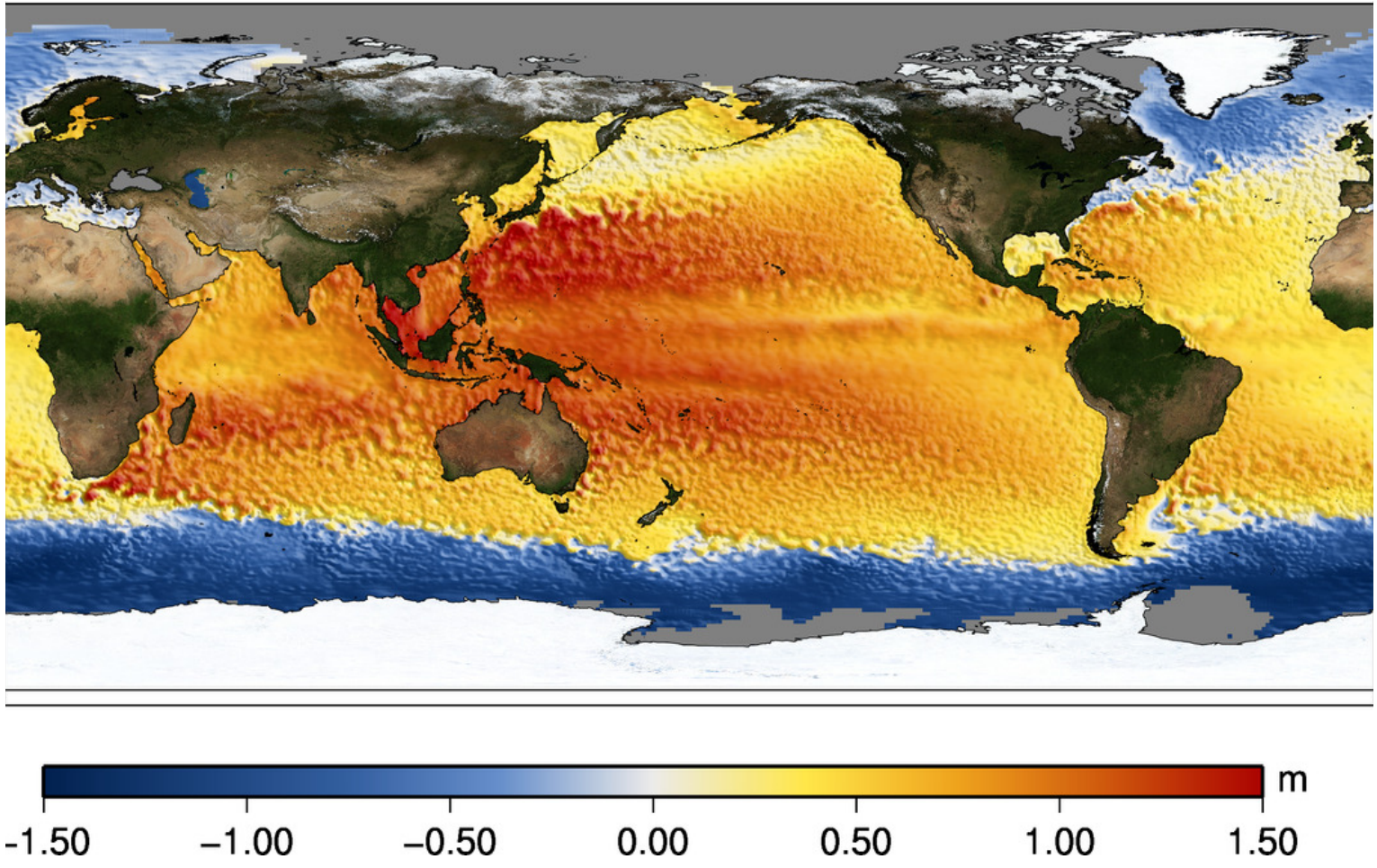

Figure 14 – Dynamic sea level on Dec. 31th 2012 (AVISO).

- Mesoscale eddies stand out in an instantaneous map !

Dynamic sea level

Exercise : estimate the typical oceanic Rossby radius of deformation. Predict how it evolves with latitude.

Definitions : $R_d = \frac{NH}{\pi f}$ *with* $N = \sqrt{-\frac{g}{\rho_0}\partial_z \rho}$ *the Brunt-Vaisala frequency,* $H \sim 5000m$ *the ocean depth,* $f \sim 10^{-4} s^{-1}$ *at mid-latitudes,* $\rho_0 = 1026 kg/m^3$ *the average density of sea water and a typical vertical stratification* $\partial_z \rho$ *of* $-5 kg/m^3$ *over the depth* H*.*

Dynamic sea level

Solution : estimated $R_d \sim 50km$ at mid-latitudes, which compares well with the observed surface eddy field. We note however that mesoscale eddies are usually larger than R_d, due to their merging by the inverse cascade of quasi-geostrophic turbulence.

R_d decreases with increasing latitude and decreasing vertical stratification, both contributing to a reduced eddy size at high latitudes. R_d can reach typically 5km at high latitude, which is a major challenge of physical oceanography because of the key role of mesoscale eddies in the circulation.

Dynamic sea level

Relation between sea level and barotropic circulation : the barotropic geostrophic balance :

$$\mathbf{k} \times \mathbf{U_g} = \mathbf{k} \times \int_{-H}^{0} \mathbf{u_g} dz = \frac{g}{f} \int_{-H}^{0} \boldsymbol{\nabla}_h \eta \, dz = \frac{gH}{f} \boldsymbol{\nabla}_h \eta = H \mathbf{k} \times \mathbf{u_{g0}}$$

Good qualitative view of the barotropic circulation because oceanic currents are surface-intensified.

Surface currents

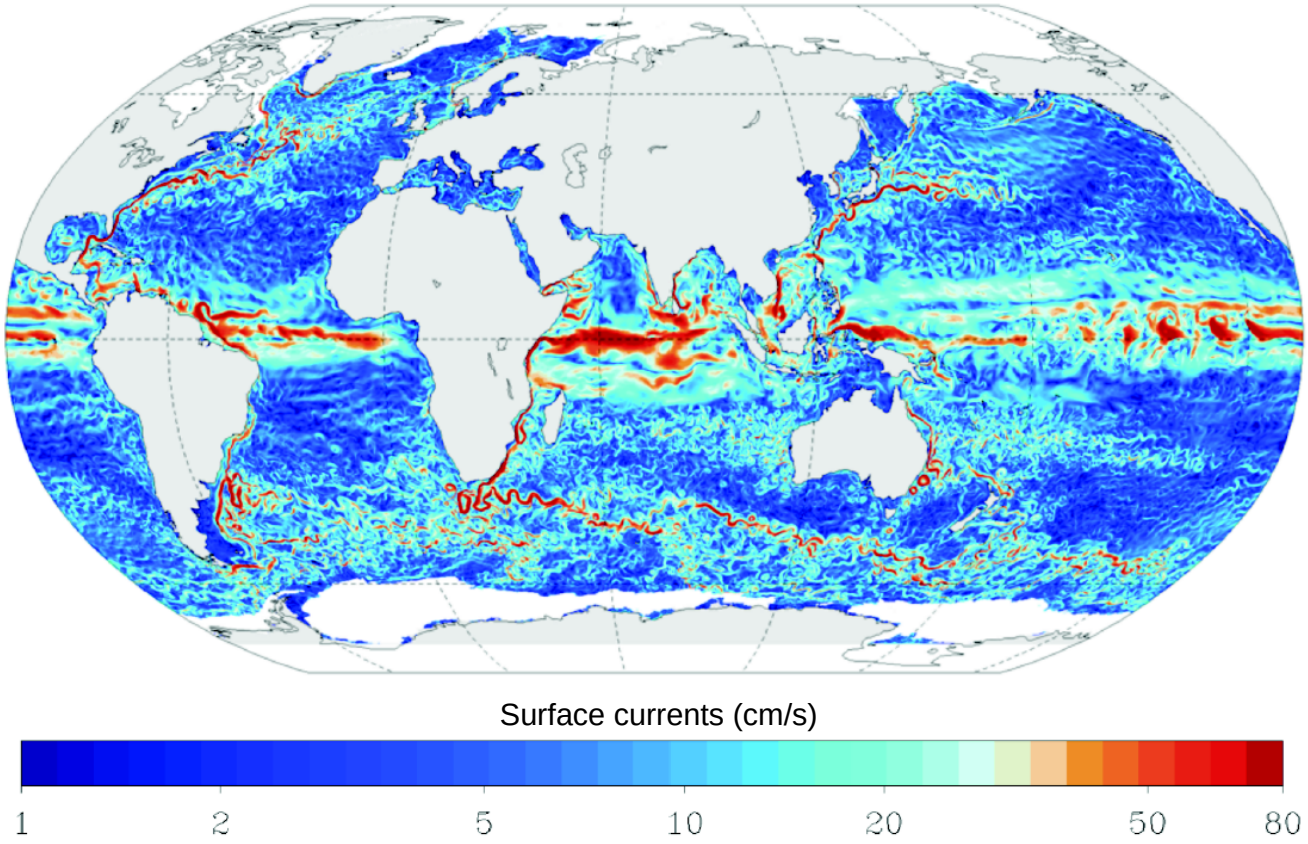

Figure 15 – Snapshot of surface currents in a $1/12^\circ$ resolution ocean simulation (Tréguier et al 2017).

Surface currents

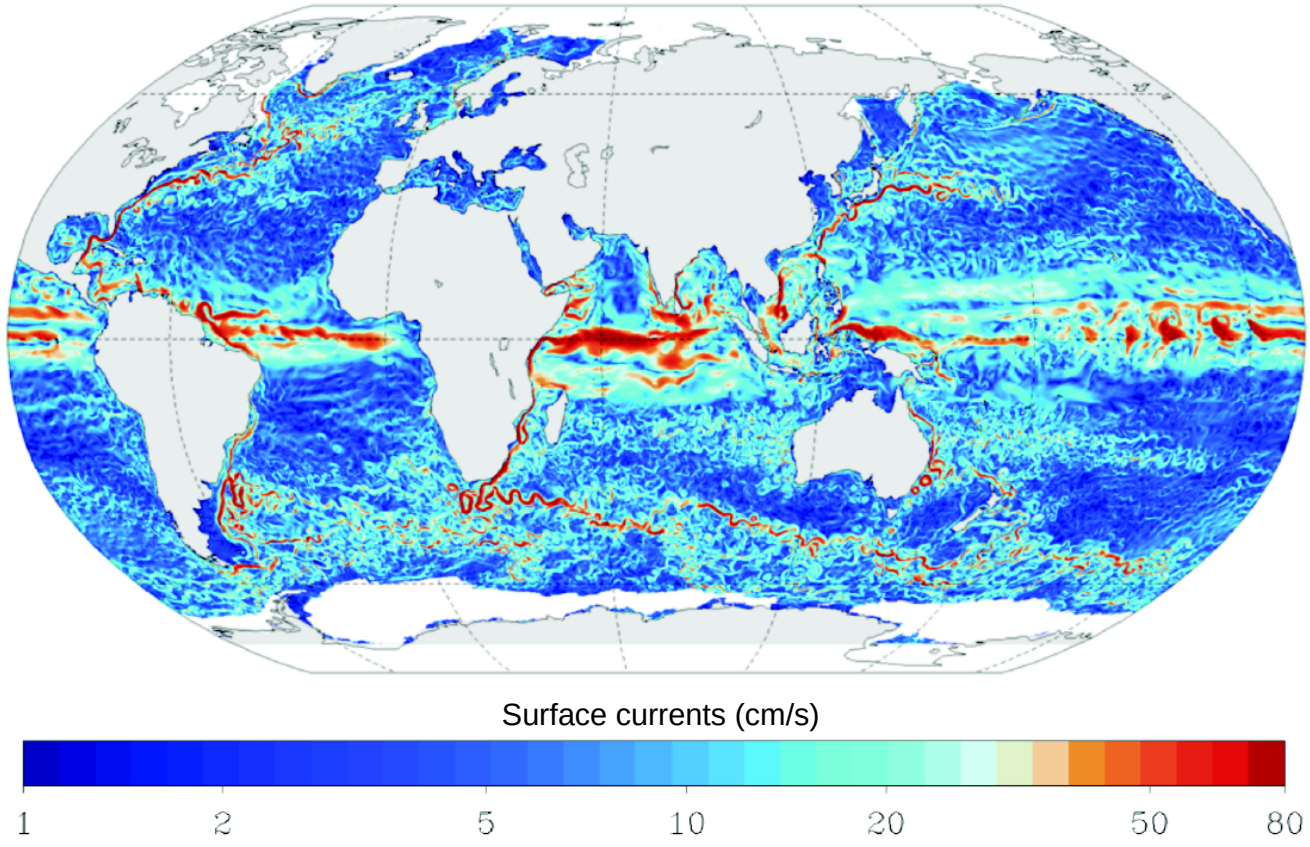

Figure 15 – Snapshot of surface currents in a 1/12° resolution ocean simulation (Tréguier et al 2017).

- Dominating currents : Western Boundary Currents, Antarctic Circumpolar Current, Equatorial currents and mesoscale eddies
- Interior gyre circulation and Eastern Boundary Currents much weaker

Surface currents

Exercise : from the typical horizontal length and velocity scales of oceanic motion, estimate the time scale of the oceanic circulation and compare it to the atmosphere.

Surface currents

Solution : $T \sim 1$ year in the ocean versus $T \sim 1$ week in the atmosphere.

- *Relative decoupling between both fluids : the ocean is felt as a relatively constant surface for atmospheric motions, and the atmosphere is felt as stochastic noise for oceanic motion.*
- *Although ocean circulation theory mostly focuses on the wind forcing, this driving force is not straightforward.*
- *A notable exception to this decoupling is in the Tropics where the oceanic response is quicker and air-sea fluxes are more intense.*

Ocean gravity waves

External tides :

- Are gravity waves excited by the Moon and Sun's gravity forces.
- Mostly ($\sim 80\%$) dissipate in shallow marginal seas by bottom friction.
- Are partly ($\sim 20\%$) converted into internal tides by interactions with topography.

Ocean gravity waves

External tides :

- Are gravity waves excited by the Moon and Sun's gravity forces.
- Mostly ($\sim 80\%$) dissipate in shallow marginal seas by bottom friction.
- Are partly ($\sim 20\%$) converted into internal tides by interactions with topography.

Internal tides :

- Are largely trapped near topography.
- Hence they generate mixing near it, where they break.
- They could have a dominant role in ventilating the abyssal ocean.

Ocean gravity waves

External wind waves :

- Are named "wind wave" when in balance with the local wind and "swell" when generated elsewhere.
- Are mostly generated below strong winds.
- Are a significant source of mixing within the surface mixed layer.

Ocean gravity waves

External wind waves :

- Are named "wind wave" when in balance with the local wind and "swell" when generated elsewhere.
- Are mostly generated below strong winds.
- Are a significant source of mixing within the surface mixed layer.

Internal wind waves :

- Are named near-inertial waves because due to the Earth rotation, their period is close to the inertial period $\frac{2\pi}{f}$.
- Are generated within the mixed layer due to wind forcing.
- Can either break within the mixed layer, or propagate below and travel long distances.
- They could also have a major role in ventilating the abyssal ocean.

Ocean gravity waves

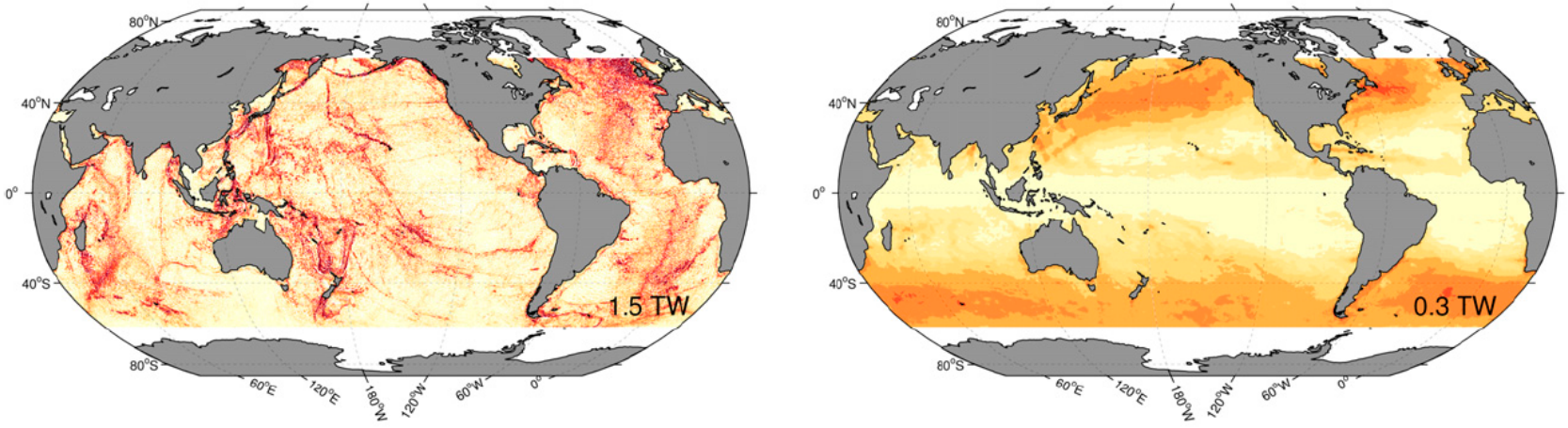

(a) Internal tides

(b) Near-inertial waves

Figure 16 – Contrasting locations for the generation of internal tides and wind (or near-inertial) waves (Waterhouse et al 2014).

- Internal tides are formed near topography.
- Internal wind waves develop below intense mid-latitude Westerly winds.

Ocean gravity waves

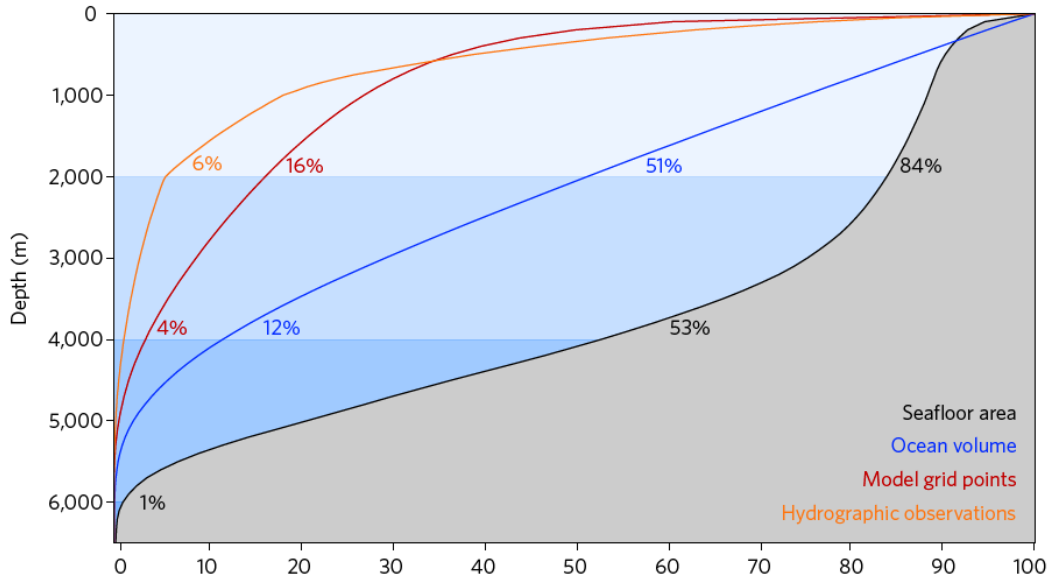

Figure 17 – On the importance of the seafloor distribution for the ocean ventilation (de Lavergne et al 2016).

- Abyssal oceans concentrate most of the interaction with topography.
- But they are by far the least observed and modelled regions.

Outline

Sea surface temperature

The main oceanic regulator of air-sea exchanges !

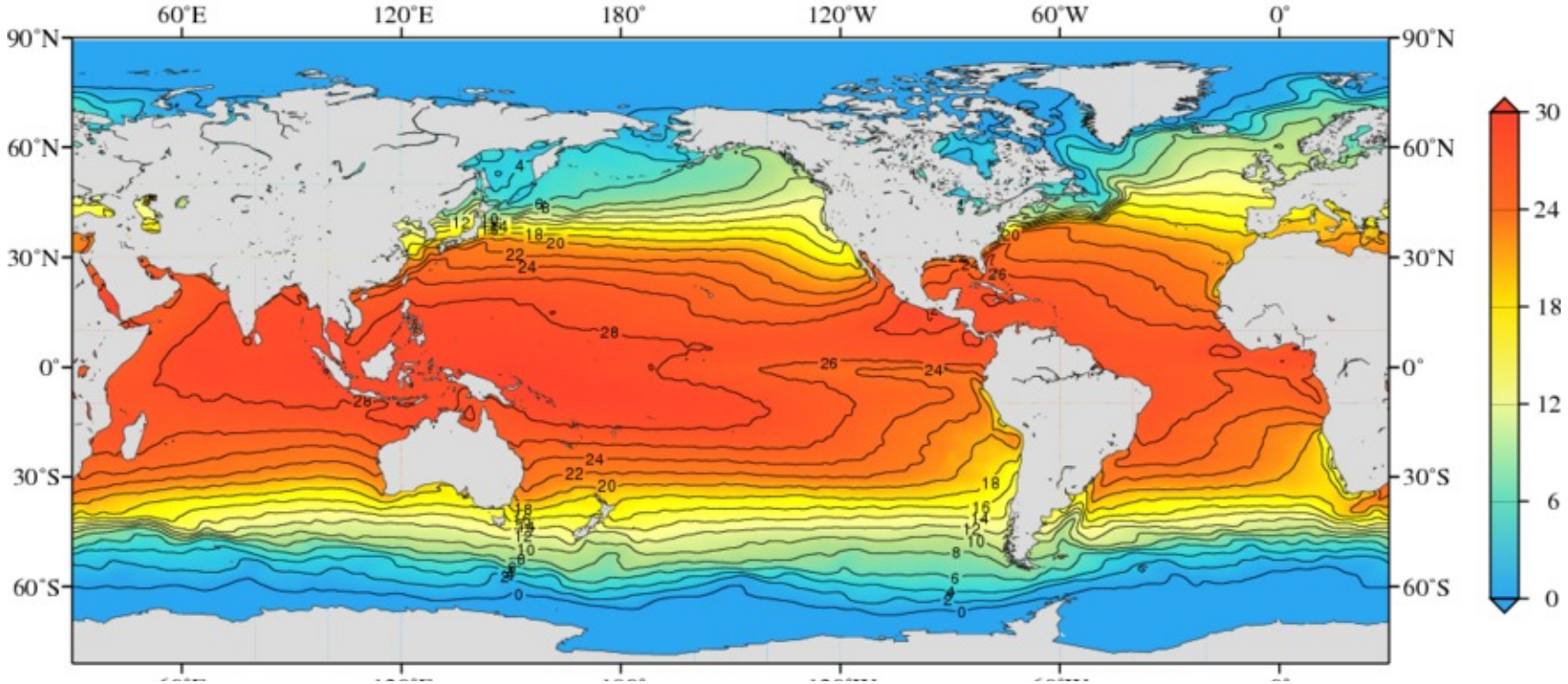

Figure 18 – 1955–2012 mean sea surface temperature in $^{\circ}C$ (WOA).

- Expected meridional gradient.
- Strong circulation-driven zonal gradients.
- Hence the ocean circulation also matters for the atmosphere !

Sea surface salinity

The second main ingredient to ocean density

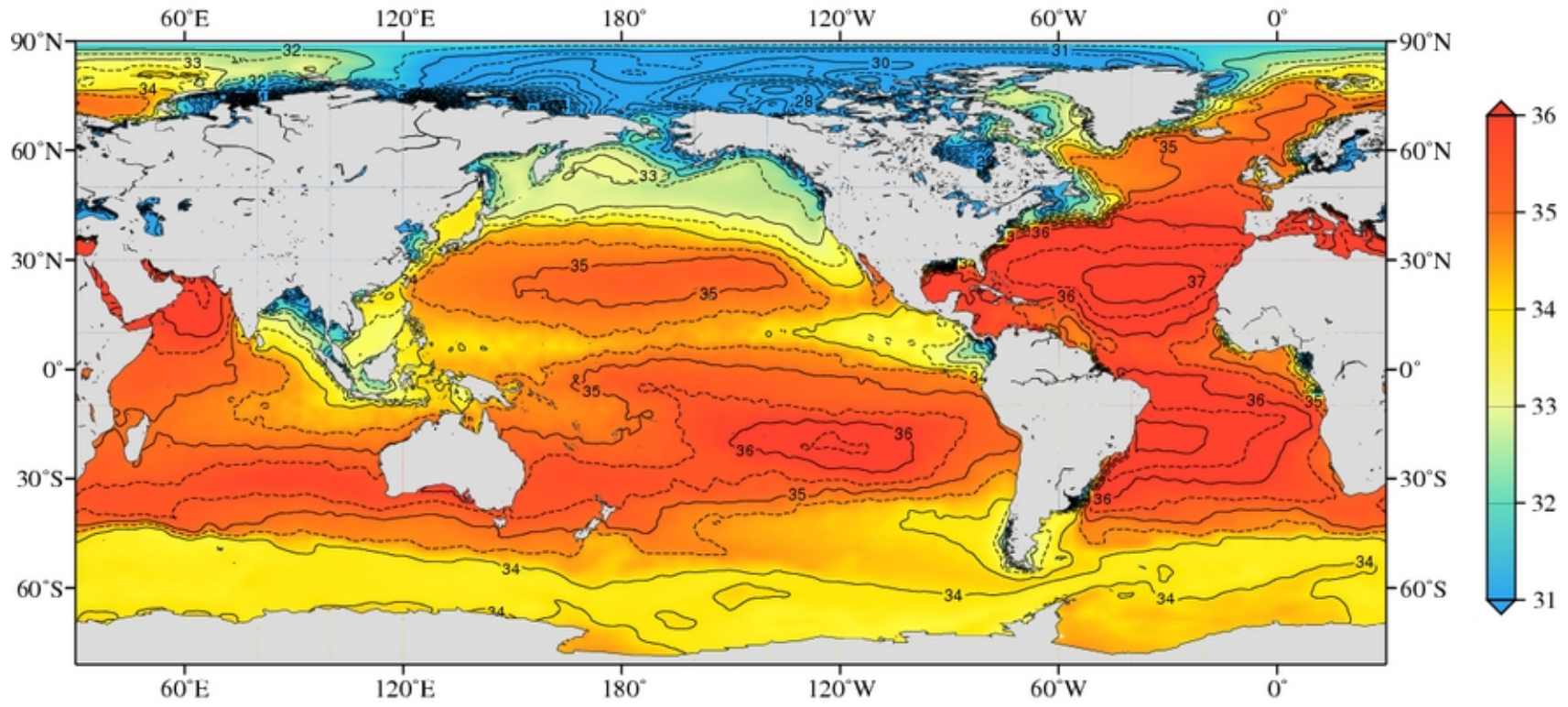

Figure 19 – 1955–2012 mean sea surface salinity (WOA).

- Circulation features appear ;
- But it mostly reflects the surface water budget ($E - P$).

Sea surface salinity

Exercise : Application of the water and salt conservation to a semi-enclosed basin with a two-way flow at its outer strait.

The Mediterranean Sea is a semi-enclosed sea connected to the Atlantic Ocean by a two-way flow at Gibraltar Strait. We know that the salinities of the incoming and outgoing waters are respectively $S_i = 36.5‰$ *and* $S_o = 38.5‰$ *and that the average net surface water flux (precipitation plus river runoff minus evaporation) within the basin is* $Q_s = -0.05 \times 10^6 m^3/s = -0.05 Sv$. *Deduce the incoming and outgoing water fluxes* Q_i *and* Q_o.

Sea surface salinity

Solution : $Q_i = +0.96Sv$ and $Q_o = -0.91Sv$, which ensures that the Mediterranean sea mass is conserved (the sea level does not fall down forever) and so is its salt (the water does not become saltier forever). This explains why fluxes between basins are generally two-way in order to equilibrate both the mass and salt budgets.

Hydrography at depth

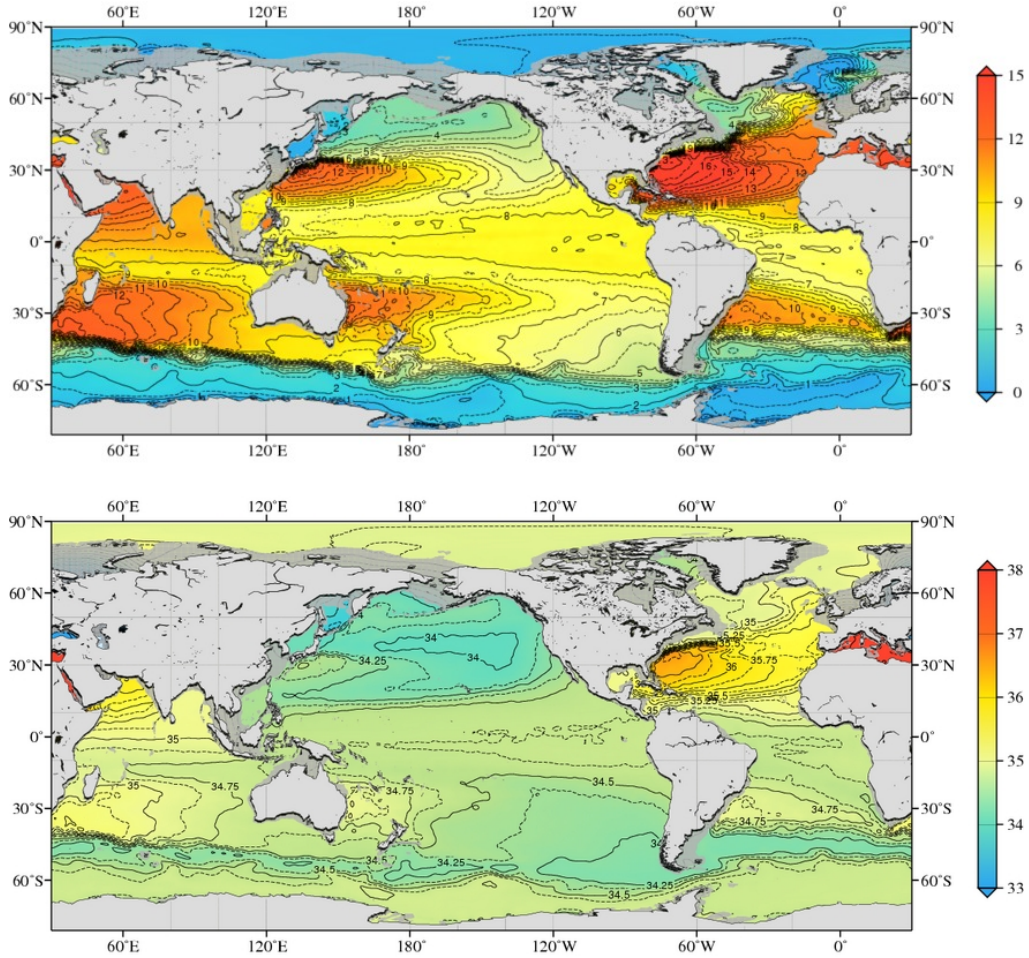

Figure 20 – 1955–2012 mean potential temperature and salinity at 500m depth (WOA).

The gyre circulation is evident on both fields : Margules's relation !

Hydrography at depth

Exercise : derive Margules's relation for a typical subtropical gyre.

We assume that the ocean is a two-layer fluid of respective densities $\rho_1 = 1022 kg/m^3$ *and* $\rho_2 = 1027 kg/m^3$ *with only the upper layer in motion, the lower layer being assumed at rest. The zonal sea level anomaly between the center and the eastern edge of the subtropical gyre is* $\Delta\eta_1 = -1m$ *over the basin width of* $L = 5000 km$*. Deduce the meridional geostrophic velocity in the upper layer and the slope of the interface* η_2 *between both layers that ensures the lower layer stays at rest.*

Hydrography at depth

Solution : $v_{g1} = -2.7 cm/s$ *and* $\Delta\eta_2 = \frac{\rho_1}{\rho_1 - \rho_2}\Delta\eta_1 = +204 m.$

- *The relatively weak southward velocity illustrates that the gyre circulation is weak in the interior ocean and results from time averaging. As illustrated before, it does not stand out clearly from instantaneous velocity fields dominated by much more energetic mesoscale dynamics.*
- *The steep interface slope permits to interpret the presence of blobs with a structure symmetric to sea level down to* $\sim 1000 m$ *depth.*

Hydrography at depth

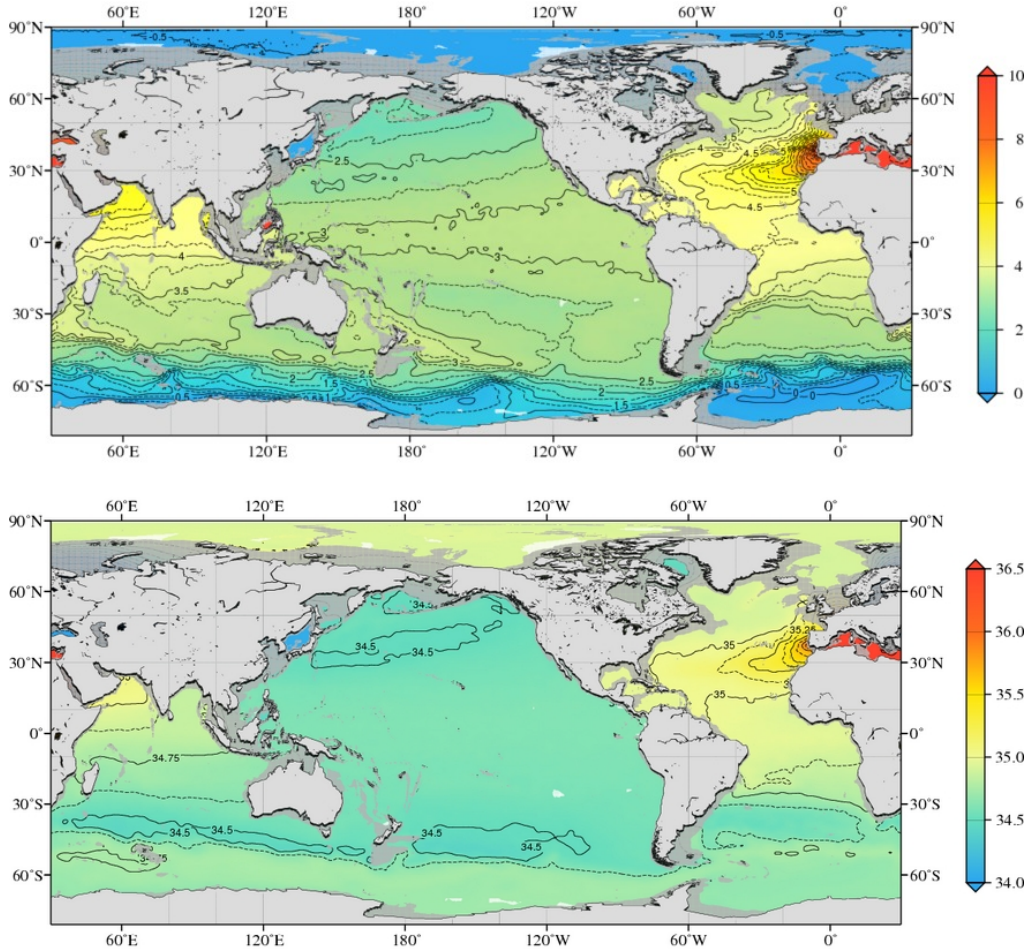

Figure 21 – 1955–2012 mean potential temperature and salinity at 1500m depth (WOA).

- Weak large-scale gradients, related to basin-scale imbalances or the thermohaline circulation activated at high latitudes.

Vertical structure

From top to bottom : mixed layer ($\sim 0-50m$), thermocline ($\sim 50-500m$) and interior/abyssal ocean ($\sim 500-5000m$).

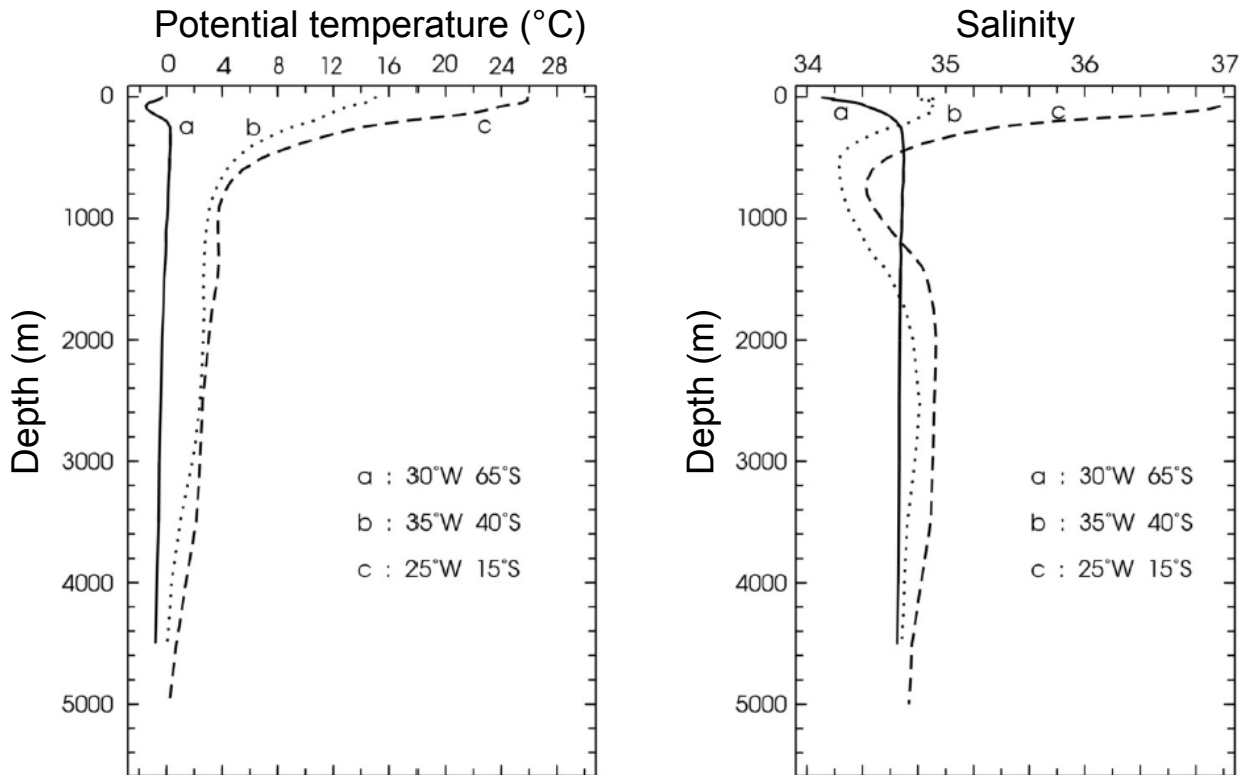

Figure 22 – Vertical hydrological profile as a function of latitude in the Southern Atlantic (Benjamin Ménétrier's lecture).

- The lower the latitude, the higher the vertical stratification !

Vertical structure

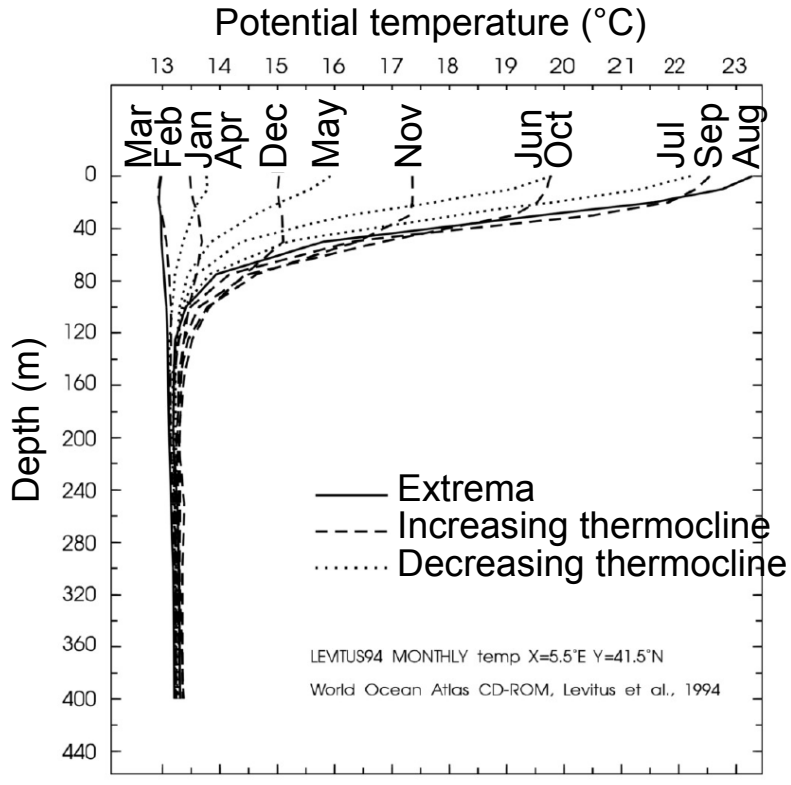

Figure 23 – Seasonal cycle of the vertical hydrological profile in a deep convection region of the Mediterranean Sea (Levitus 1994 and BM's lecture).

- Strong seasonal cycle of the sea surface temperature and mixed layer.
- Interior water masses are formed in winter by deep convection.

Vertical structure

Exercise : what air-sea heat flux Q_0 (in J/m^2) is required to cool down a mixed layer of $h = 50m$ depth by $1^\circ C$? By how many degrees would this flux heat a surface atmospheric layer of the same height ? What are the consequences for oceanic static stability ?

The heat capacities at constant pressure are respectively $c_w = 3993 J/K/kg$ and $c_a = 1005 J/K/kg$, with respective densities of $\rho_w = 1025 kg/m^3$ and $\rho_a = 1.2 kg/m^3$.

Vertical structure

Solution : $Q_0 = 1 \times h \times \rho_w \times c_w = 204.6 MJ/m^2$ *and* $\Delta T_a = \frac{Q_0}{h \times \rho_a \times c_a} = +3396.4^\circ C$.

- *It is mostly the large difference in densities between sea and air (and partly the higher heat capacity per unit mass) that explains the relative decoupling between both components and why the ocean is a slowly-evolving component of the climate system.*
- *In the ocean, a surface cooling induces a static instability at the basis of the mixed layer, where colder waters are above warmer waters. This triggers oceanic convection towards the bottom, which deepens the mixed layer.*

Outline

Surface heat fluxes

Shortwave radiative heat flux :

- The main source of energy for the ocean
- $Q_{SW} = F_s cos(V_s) T_a (1 - \alpha)$
  with F_s the solar constant, V_s the solar zenith angle, T_a the proportion transmitted by the atmosphere and $\alpha \simeq 0.06$ the ocean albedo
- Main dependencies : latitude and seasonal/diurnal cycles, cloudiness and presence of sea ice.

Surface heat fluxes

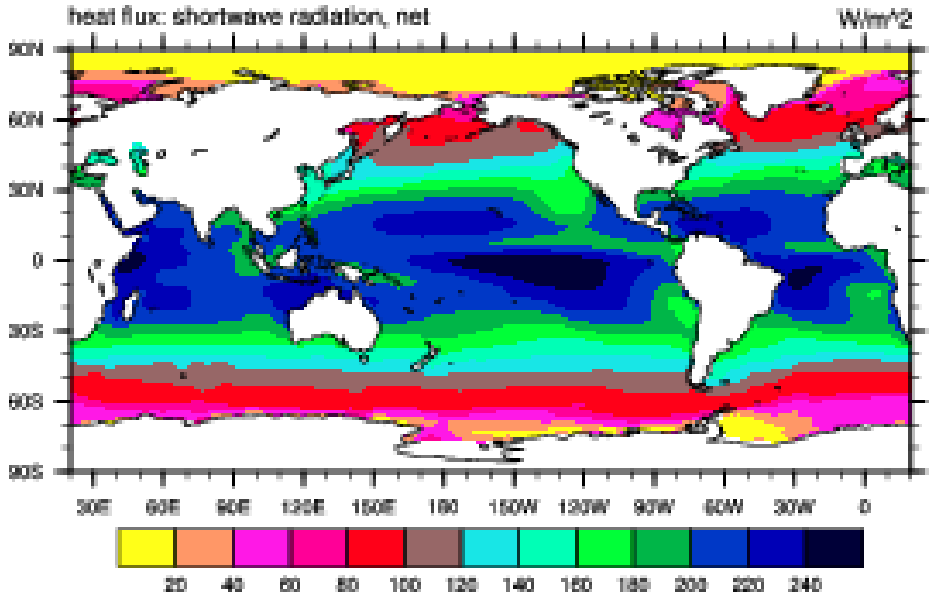

Figure 24 – 1984–2006 average net shortwave heat flux at the air-sea interface from an atmospheric reanalysis (CORE2/NCAR).

- General meridional gradient, enhanced at mid-latitudes
- Minimum along the ITCZ and eastern boundaries

Surface heat fluxes

Longwave radiative heat flux :

- Represents $\sim 1/3$ of the oceanic heat loss
- $Q_{LW} = (1 - \alpha_{LW})\varepsilon_a \sigma T_a^4 - \varepsilon_o \sigma SST^4$
  with $\alpha_{LW} \simeq 0.045$ the ocean longwave albedo, σ the Stephan-Boltzmann constant, ε_a (very variable) and $\varepsilon_o \simeq 0.97$ the air and sea emissivities.
- Main dependencies : air-sea temperature difference, atmospheric cloud and vapour content and presence of sea ice.

Surface heat fluxes

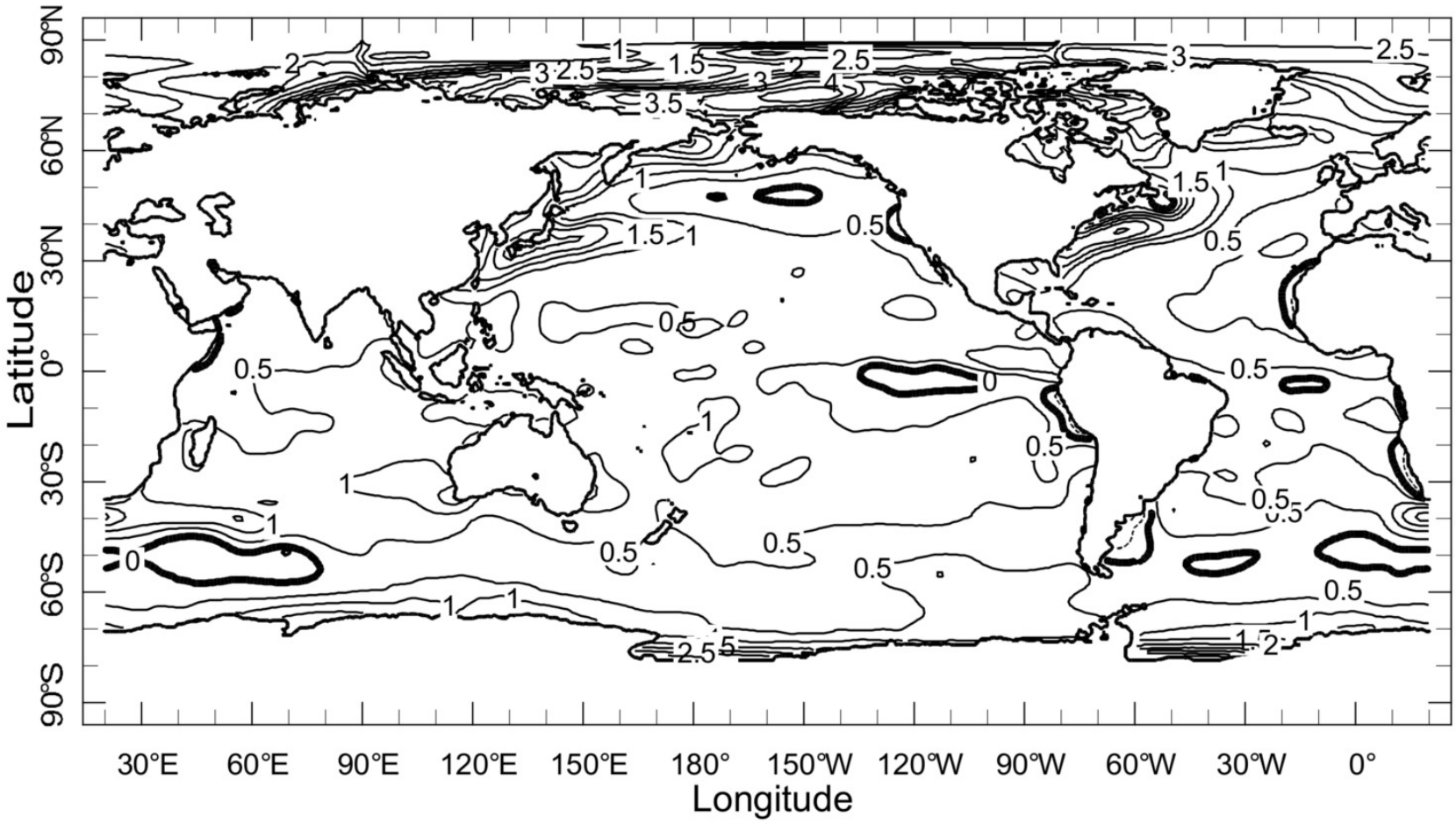

Figure 25 – Annual mean sea-air temperature difference ($^{\circ}C$, BM's lecture).

- Surface ocean warmer than surface atmosphere.

Surface heat fluxes

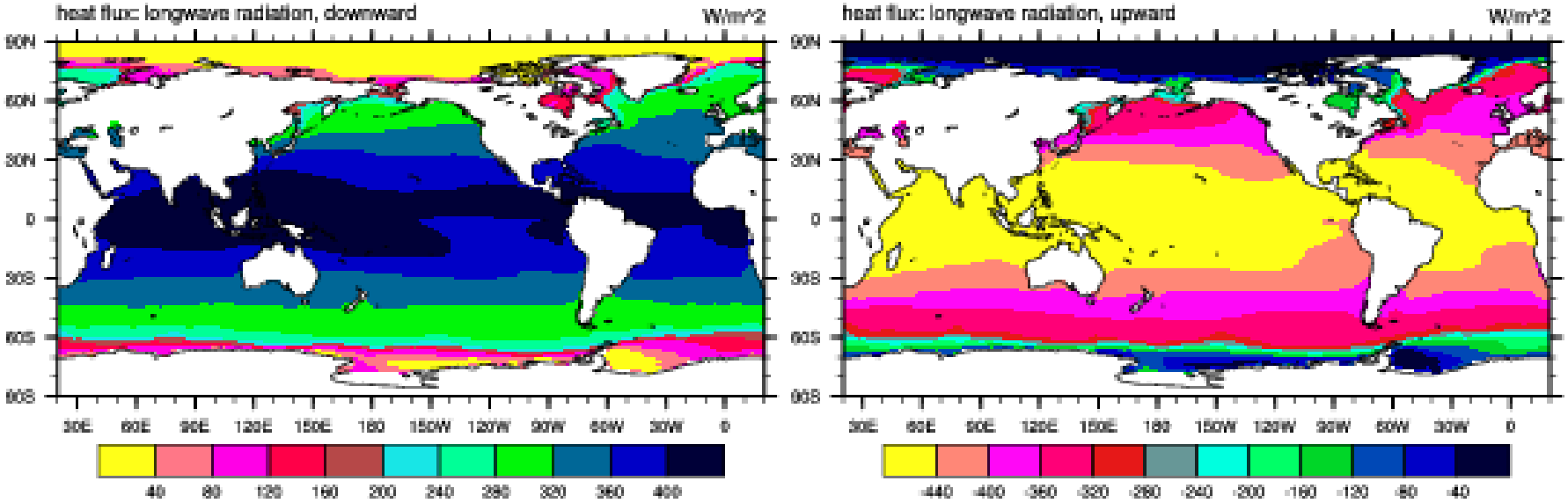

Figure 26 – 1984–2006 average downward and upward longwave heat fluxes at the air-sea interface from an atmospheric reanalysis (CORE2/NCAR).

- Large compensation between downward and upward longwave heat fluxes.
- Maximum net longwave heat loss in the Subtropics : low cloudiness and humidity.

Surface heat fluxes

Turbulent heat fluxes :

- Outside of a millimetric surface boundary layer, air-sea heat and water exchanges are mostly advective.
- This small-scale advection is modelled by a "Reynolds decomposition" as turbulent vertical fluxes : $\overline{w'\theta'}$ and $\overline{w'q'}$.
- Those exchanges are unresolved by numerical models and poorly observed.
- Parametrized by so-called "Bulk aerodynamic formulas" from the Monin Obukhov Similarity Theory (MOST).
- Include the sensible Q_S and latent Q_L heat fluxes.

Surface heat fluxes

Sensible heat fluxes :

- Weak negative contribution to the global net air-sea exchanges.
- $Q_S = -\rho_a c_a C_\theta |\mathbf{U(10m)}|(SST - \theta_a(2m))$
  with C_θ an empirical transfer coefficient, $|\mathbf{U(10m)}|$ the wind module at 10m height, $\theta_a(2m)$ the air temperature at 2m height.
- Main dependencies : air-sea temperature difference plus wind, surface roughness and atmospheric stability that modulate C_θ.

Surface heat fluxes

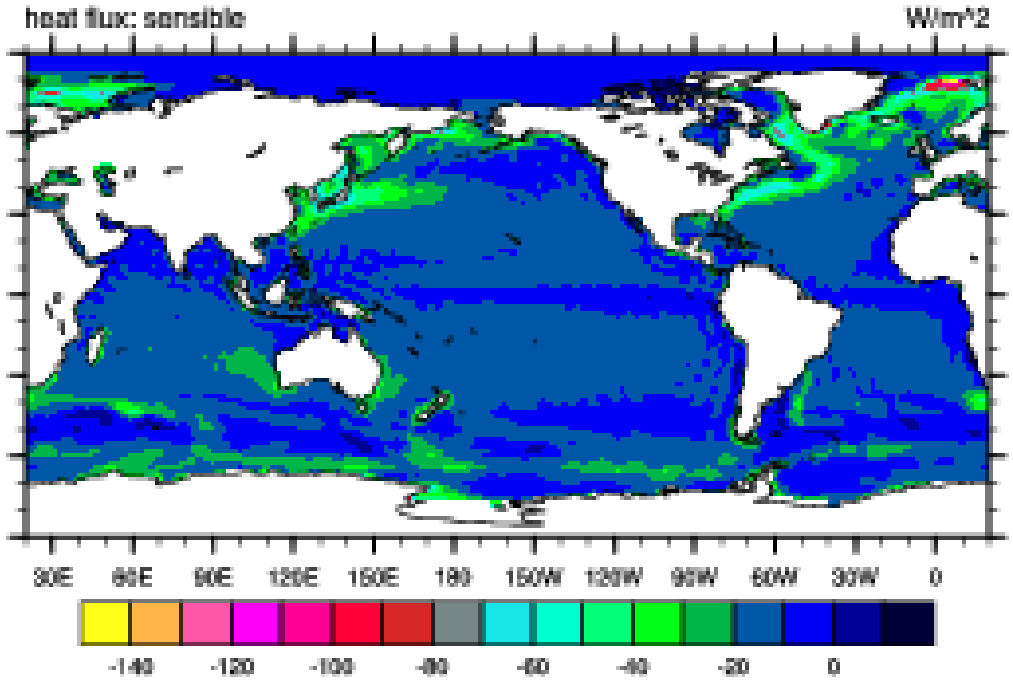

Figure 27 – 1984–2006 average sensible heat flux at the air-sea interface from an atmospheric reanalysis (CORE2/NCAR).

- Mostly weakly negative.
- Largely negative at western boundaries and high latitudes where $(SST - \theta_a(2m))$ is largest.

Latent heat fluxes :

- The main oceanic heat sink ($\sim 2/3$).
- $Q_L = -\rho_a L_v C_q |\mathbf{U(10m)}| (0.98 q^*(P_0, SST) - q(2m))$ with C_q an empirical transfer coefficient, $q(2m)$ the specific humidity at 2m height, $0.98 q^*(P_0, SST)$ the specific humidity at surface which is equal to the saturating humidity (the factor 0.98 is due to ocean salinity).
- Main dependencies : air-sea humidity difference (depending on air temperature and humidity) plus wind, surface roughness and atmospheric stability that modulate C_q.

Surface heat fluxes

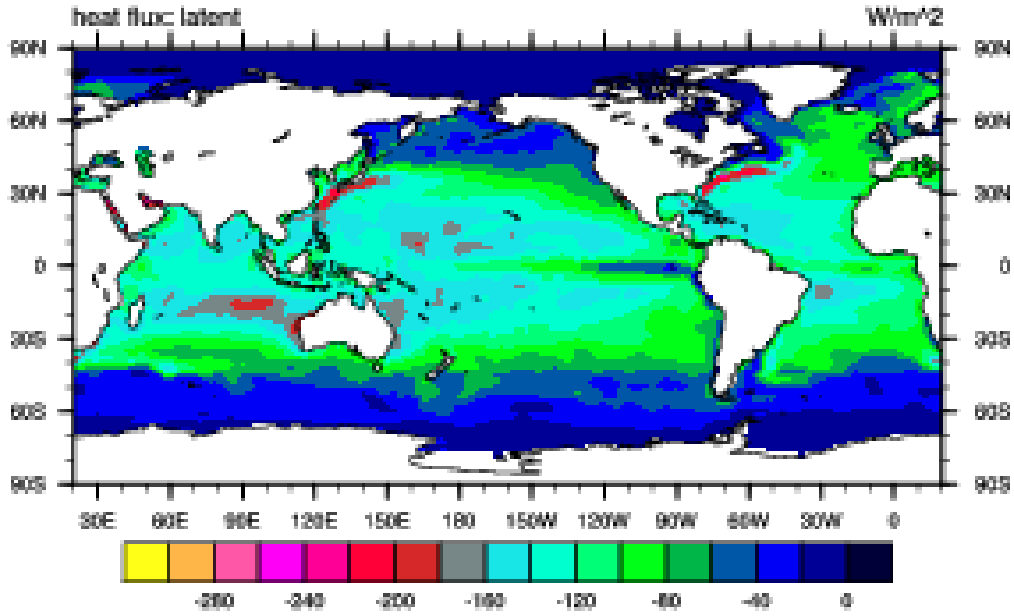

Figure 28 – 1984–2006 average sensible heat flux at the air-sea interface from an atmospheric reanalysis (CORE2/NCAR).

- Strictly negative by definition.
- Similar patterns to Q_S : mostly negative where strong cold and/or dry winds blow over warm sea surface temperatures.

Surface heat fluxes

Total net heat flux :

$$Q_0 = Q_{SW} + Q_{LW} + Q_S + Q_L$$

Surface heat fluxes

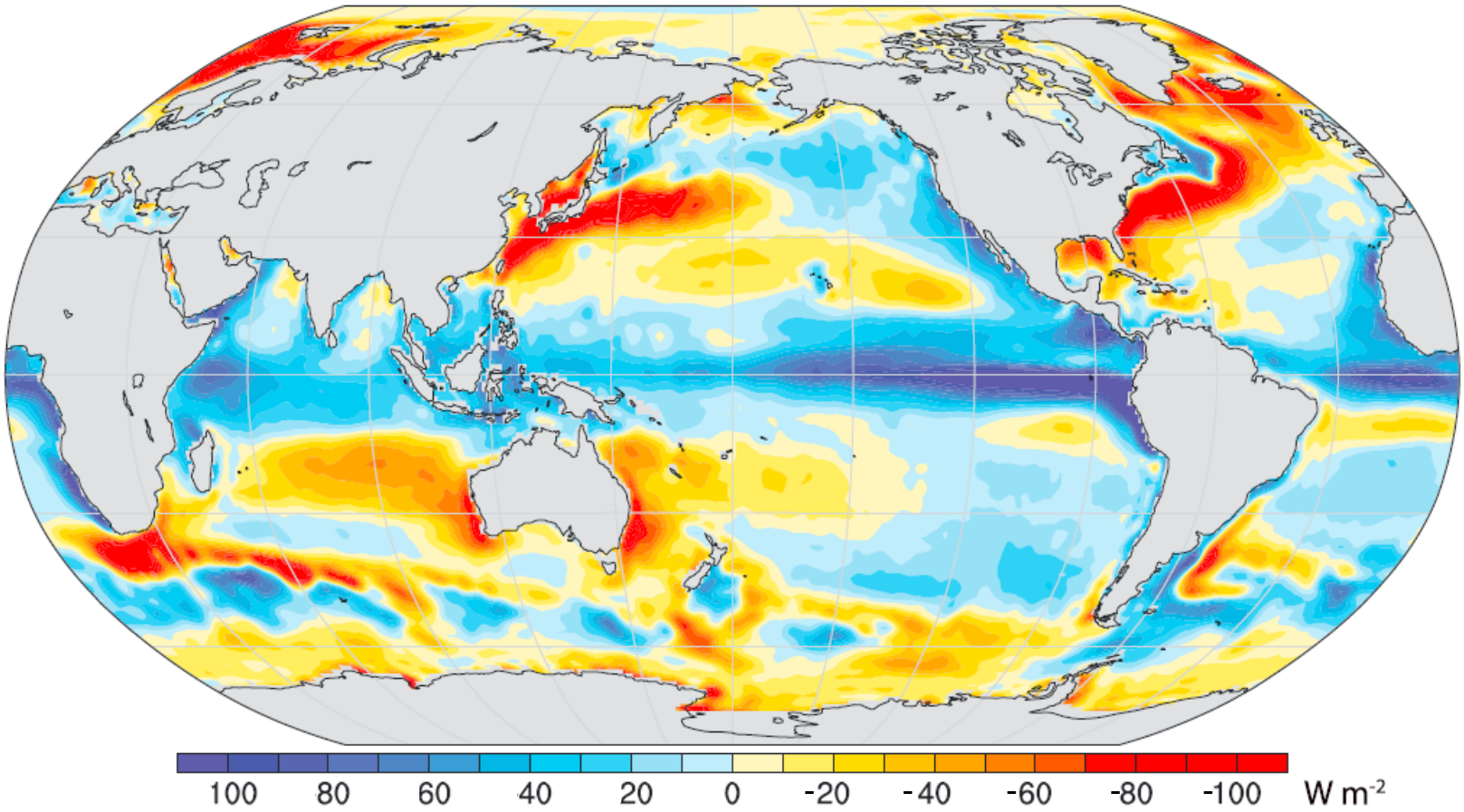

Figure 29 – 2000–2014 average total net air-sea heat flux (Trenberth and Fasullo 2017).

- Globally balanced : current radiative forcing $\simeq +0.8 W/m^2$.
- The ocean warms in the Tropics and cools at higher latitudes.
- Hence ocean circulation transports heat poleward !

Surface heat fluxes

Exercise : qualitatively, what negative feedbacks in the air-sea fluxes occur if Q_{SW} increases ? What if the SST increases ?

Surface heat fluxes

Solution :

- *The increase in Q_{SW} will induce a negative feedback of all three other air-sea heat fluxes through its impact on SST. Indeed, a warmer SST will cause larger upward Q_{LW} (grey body law), more Q_S toward the atmosphere ($T_a - SST$ more negative) and higher Q_L (higher q_s^* at higher temperature).*
- *The increase in SST will similarly increase these three heat fluxes, which will also act as a negative feedback. In addition, increased atmospheric convection above a warm SST will increase cloudiness and hence reduce Q_{SW}.*
- *In both case, a new and warmer climate balance will be reached which closes the surface heat budget.*

Surface momentum fluxes

- Also turbulent fluxes $\overline{w'u'}$ and $\overline{w'v'}$ parametrized by "Bulk aerodynamic formulas" deduced from MOST.
-

$$\begin{aligned} \tau_0 &= \rho_a C_d |\mathbf{U(10m)} - \mathbf{u_o}| (\mathbf{U(10m)} - \mathbf{u_o}) \\ &\simeq \rho_a C_d |\mathbf{U(10m)}| \mathbf{U(10m)} \end{aligned}$$

  with C_d an empirical transfer coefficient and $\mathbf{u_o}$ surface currents.
- Main dependencies : mostly wind but also : surface roughness and atmospheric stability that modulate C_d, and $\mathbf{u_o}$.

Surface momentum fluxes

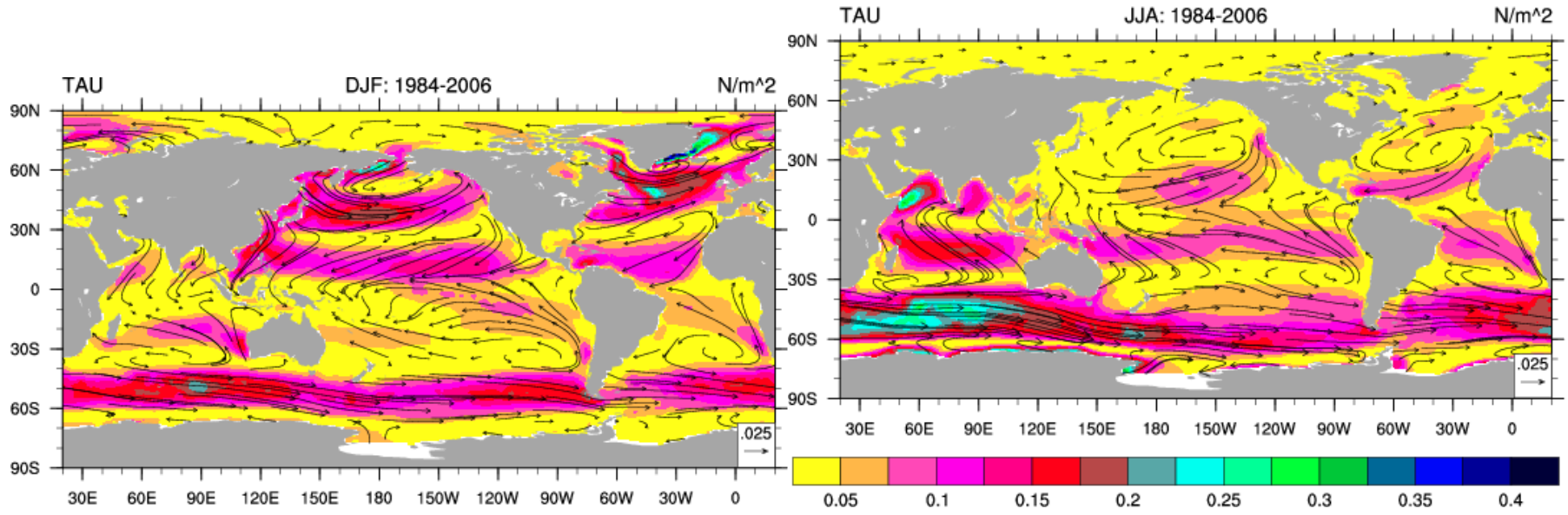

Figure 30 – 1984–2006 average momentum flux at the air-sea interface (wind stress) for the boreal and austral winters from an atmospheric reanalysis (CORE2/NCAR).

- Mid-latitude westerlies and tropical trade winds stand out.
- Strong weasonal cycle.

Surface water fluxes

- $F_W = -E + P + R$
  with E evaporation ($-1.2 m/y$), P precipitation ($+1.1 m/y$) and R mostly river runoff ($+0.1 m/y$)
- Other minor contributions can add up to the runoff : water-ice transformations (ice shelves, glacier and iceberg melting, sea ice formation/melting) and underground river discharges. The former contrubites to $\sim 2/3$ ($\sim +2 mm/y$) of current sea level rise.

Surface water fluxes

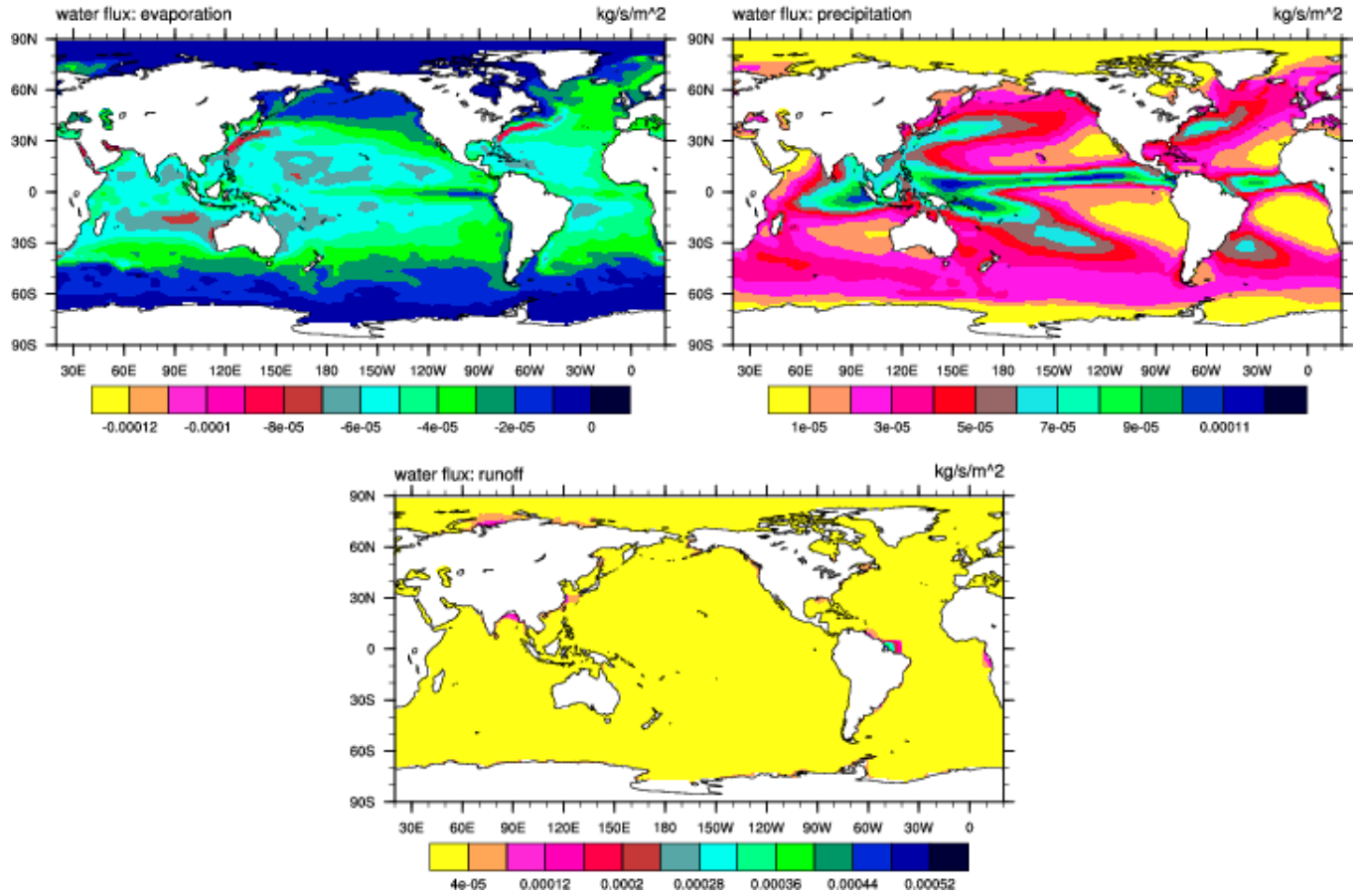

Figure 31 – 1984–2006 average evaporation, precipitation and river runoff at the air-sea interface from an atmospheric reanalysis (CORE2/NCAR).

- Evaporation : in the Subtropics.
- Precipitation : along the ITCZ and poleward of the Subtropics.
- Runoff : very coastal and largest in the Tropics.

The ocean and Earth heat balance

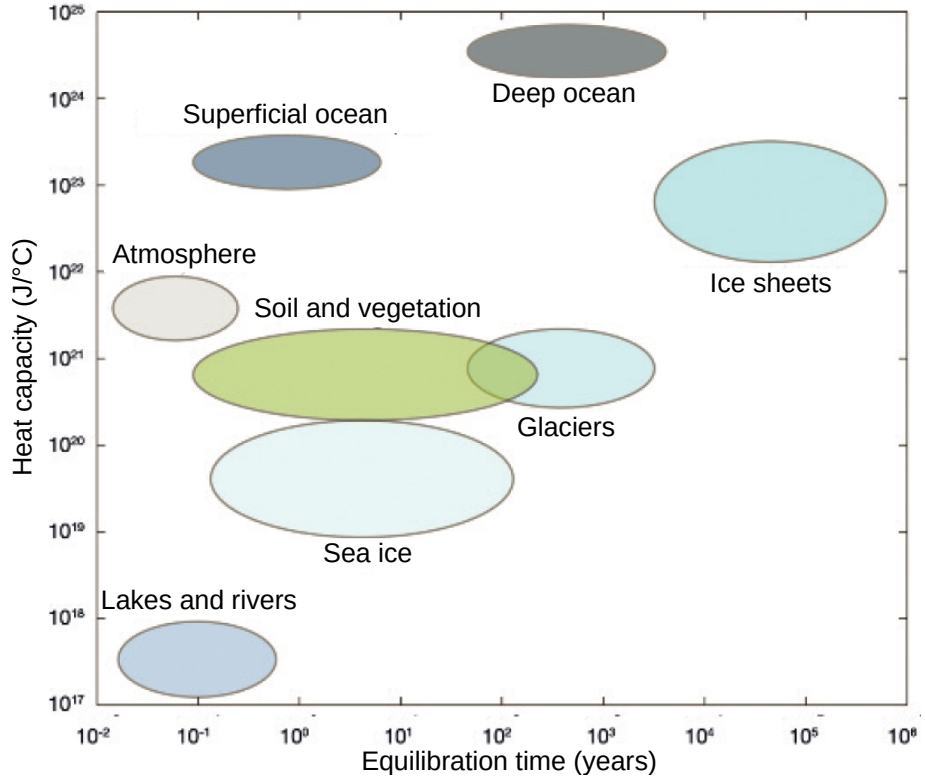

Figure 32 – Diagram of the heat capacity and equilibration time of the main climate components (de Lavergne 2018).

- The ocean is by far the main thermodynamic reservoir of the climate system.
- It has stored $> 90\%$ of the anthropogenetic global warming.

The ocean and Earth heat balance

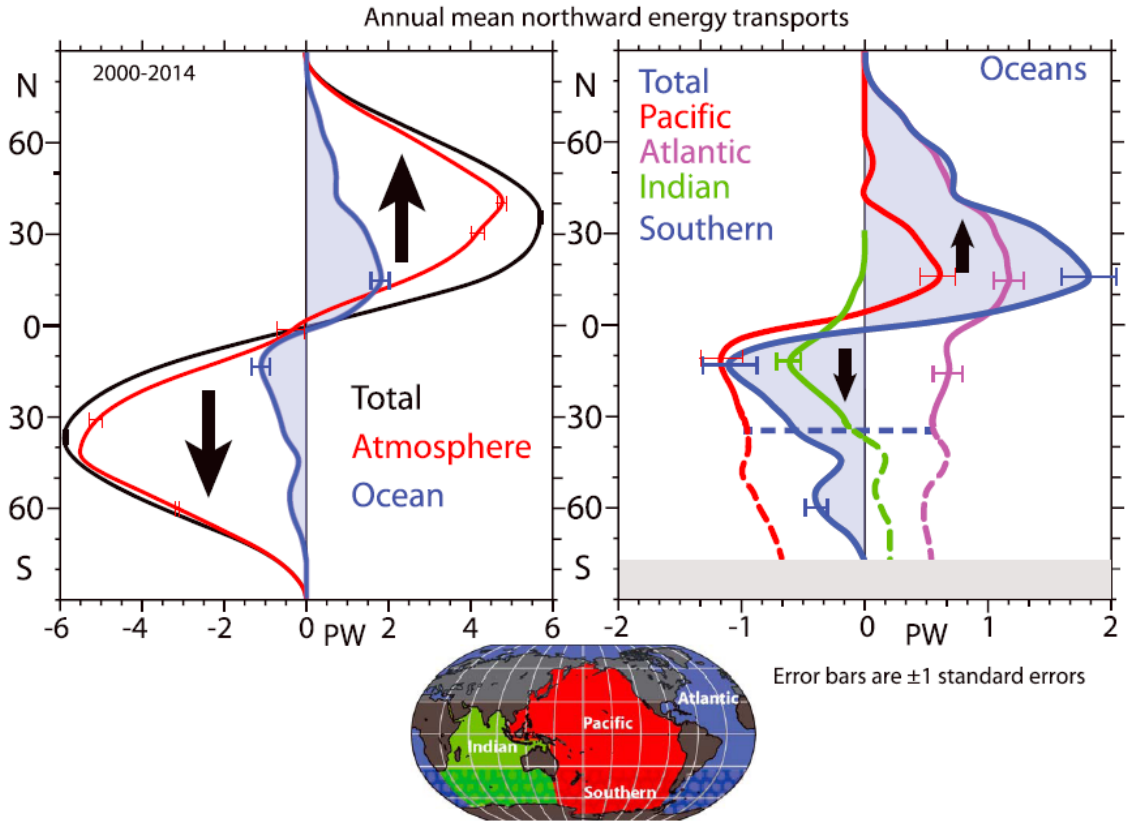

Figure 33 – 2000–2014 average meridional heat transport for the atmosphere and ocean, and per main oceanic basinc (Trenberth and Fasullo 2017).

- The atmosphere dominates except in the Tropics.
- The ocean represents $\sim 1/4$ of the meridional heat transport.
- The Atlantic and Pacific dominate respectively the NH and SH.

The ocean and Earth heat balance

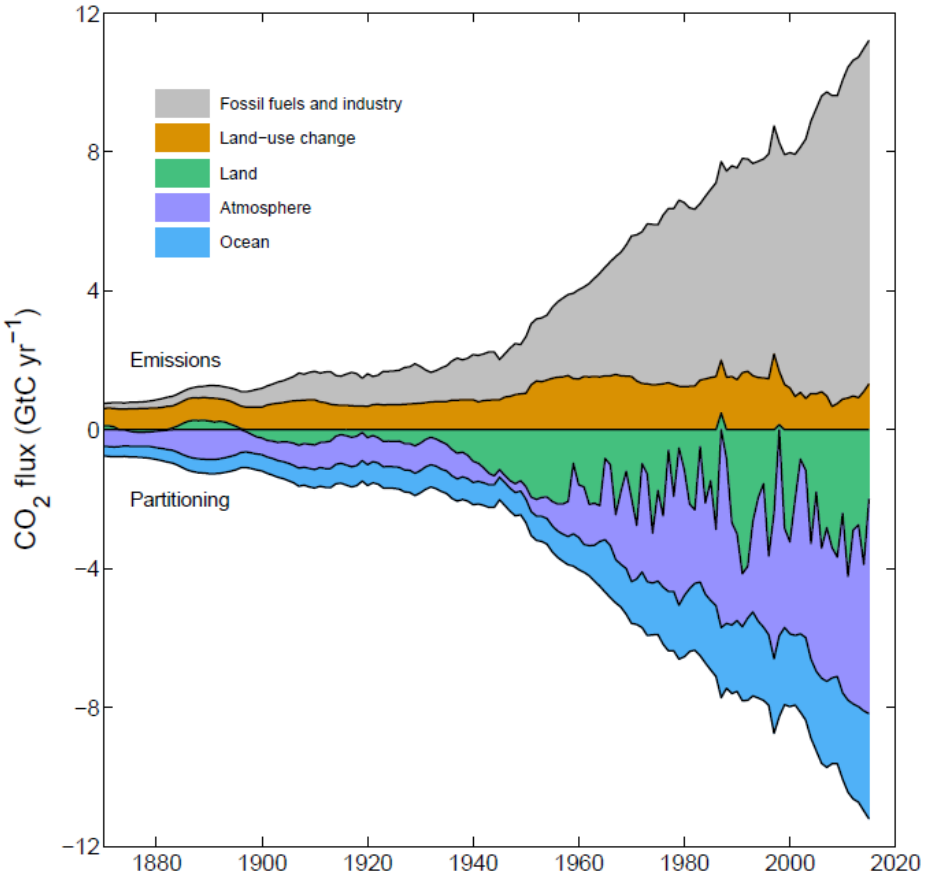

Figure 34 – Inventory of the annual emission and storage rate of CO_2 (Le Quéré et al 2016).

The ocean has stored $\sim 1/4$ of the anthropogenetic CO_2.